TÉCNICO LISBOA

Underwater Optical Communication for Cooperative Autonomous Marine Vehicles

Ayesha Aslam

Thesis to obtain the Master of Science Degree in

Electrical and Computer Engineering

Supervisors: Prof. David Alexandre Cabecinhas
Prof. Pedro J. Sanz

Examination Committee

Chairperson: Prof. António Manuel Raminhos Cordeiro Grilo
Supervisor: Prof. David Alexandre Cabecinhas
Member of the Committee: Prof. Bruno Duarte Damas

November 2024

This work was created using LaTeX typesetting language
in the Overleaf environment (www.overleaf.com).

Declaration

I declare that this document is an original work of my own authorship and that it fulfills all the requirements of the Code of Conduct and Good Practices of the Universidade de Lisboa.

Acknowledgments

I would like to extend my heartfelt gratitude to my supervisor at UJI, Professor Pedro J. Sanz, for his invaluable guidance and support throughout the thesis research. His expertise, particularly in the control of underwater autonomous vehicles, has been instrumental in shaping the direction of this work. I would also like to express my deep appreciation to Professor Raul Marín Prades, as a personal mentor, for his continuous advice, and help with the optical modems. His mentorship has been a guiding light throughout my research journey. I am also profoundly grateful to my co-supervisor, Professor Dr. David Cabecinhas, for his expertise, patience, and constructive criticism, which have significantly contributed to the quality of my work.

To my mother, whose support and encouragement have been my pillar of strength throughout this journey. Her resilience and unwavering faith in me have inspired and motivated me to reach this milestone. This work stands as a testament to her love and guidance.

I would also like to acknowledge Jaume I University for the financial support that made this research possible, as well as CIRTESU (Centro de Investigación en Robótica y Tecnología Subacuática) for providing access to the necessary resources and facilities that were essential to conducting my research.

Finally, I dedicate this Master's thesis to Allah, my father, and my siblings, for their constant prayers and belief in me. To my dear nephew, Mustafa, who inspires me with his boundless curiosity, I dedicate this work to him with the hope that his future is filled with as much wonder and excitement as he brings into our lives every day.

Last but not least, to my fiancé, Nafeel, who helped me grow and was always there for me during the good and bad times. I cannot thank him enough for his love, patience, and encouragement. This accomplishment is as much his as it is mine, and I am forever grateful to have him by my side.

To each and every one of you —thank you.

Abstract

The field of underwater robotics is evolving rapidly, with applications ranging from exploration to environmental monitoring. This thesis investigates the use of optical communication and leader-follower control in multi-agent systems to enhance underwater vehicle coordination. Focusing on the BlueROV2 platform, this research integrates LUMA™ optical modems to establish a robust, high-bandwidth communication link between leader and follower vehicles, enabling precise formation control in underwater environments. The study includes the development of custom ROS packages for direct modem configuration via the Linux terminal, the creation of a control algorithm for coordinated movement, and the implementation of a simulation environment using MATLAB to validate the system's functionality under controlled conditions. Simulation tests conducted across diverse scenarios evaluate the performance, reliability, and adaptability of the optical modems. This work contributes to the field by presenting a high-speed, low-latency communication system for multi-robot underwater operations, offering advancements in coordinated marine exploration and research.

Keywords

Underwater robotics, BlueROV2, multi-agent systems, leader-follower control, optical communication, LUMA™ modems, ROS, MATLAB, coordinated marine exploration.

Resumo

O domínio da robótica subaquática está a evoluir rapidamente, com aplicações que vão da exploração à monitorização ambiental. Esta tese investiga a utilização da comunicação ótica e do controlo líder-seguidor em sistemas multi-agente para melhorar a coordenação de veículos subaquáticos. Centrando-se na plataforma BlueROV2, esta investigação integra modems ópticos LUMA™ para estabelecer uma ligação de comunicação robusta e de elevada largura de banda entre os veículos líder e seguidor, permitindo um controlo preciso da formação em ambientes subaquáticos. O estudo inclui o desenvolvimento de pacotes de software ROS para a configuração direta do modem através de um terminal Linux, a criação de um algoritmo de controlo para o movimento coordenado e a implementação de um ambiente de simulação utilizando o MATLAB para validar a funcionalidade do sistema em condições controladas. Os testes de simulação realizados em diversos cenários avaliam o desempenho, a fiabilidade e a adaptabilidade dos modems ópticos. Este trabalho contribui para a a literatura do campo ao apresentar um sistema de comunicação de alta velocidade e baixa latência para operações subaquáticas multi-robô, oferecendo avanços na exploração e investigação marinha coordenada.

Palavras Chave

Robótica subaquática, BlueROV2, sistemas multi-agente, controlo líder-seguidor, comunicação ótica, modems LUMA™, ROS, MATLAB, exploração marinha coordenada.

Contents

List of Figures

List of Tables

Acronyms

- **AGC** Auto-Gain Control
- **API** Application Programming Interface
- **APF** Artificial Potential Field
- **AUV** Autonomous Underwater Vehicle
- **CG** Center of Gravity
- **CIRTESU** Centre for Research in Robotics and Underwater Technologies
- **CO** Center of Origin
- **CSAIL** Computer Science and Artificial Intelligence Laboratory
- **DLOS** Diffused Line-of-Sight
- **DOF** Degrees of Freedom
- **FSO** Free-Space Optics
- **H2** Performance measure for optimal control in system theory
- **IMU** Inertial Measurement Unit
- **IP** Internet Protocol
- **LD** Laser Diode
- **LED** Light Emitting Diode
- **LOS** Line-of-Sight
- **LUMA** Optical modem brand by Hydromea
- **MER** Mars Exploration Rovers

- **MIT** Massachusetts Institute of Technology
- **MORPH** Marine Robotic System of Self-Organizing, Logically Linked Physical Nodes
- **MPC** Model Predictive Control
- **MPPC** Multi-Pixel Photon Counter
- **NED** North East Down
- **NLOS** Non-Line-of-Sight
- **OFDM** Orthogonal Frequency Division Multiplexing
- **PAM4** Pulse Amplitude Modulation 4-Level
- **POF** Plastic Optical Fiber
- **QAM** Quadrature Amplitude Modulation
- **RF** Radio Frequency
- **RLOS** Retro-Reflector-Based Line-of-Sight
- **ROBOVOLC** Robotic Exploration of Volcanic Areas
- **ROM** Read-Only Memory
- **ROS** Robot Operating System
- **ROV** Remotely Operated Vehicle
- **RS232**/**RS485** Serial Communication Standards
- **SNAME** Society of Naval Architects and Marine Engineers
- **TDMA** Time Division Multiple Access
- **UAV** Unmanned Aerial Vehicle
- **UWOC** Underwater Wireless Optical Communication
- **UWSN** Underwater Wireless Sensor Network
- **WiMUST** Widely-Integrated Marine Unmanned Systems Technologies

1

Introduction

Contents

1.1 Background and Motivation

In recent decades, technological advancements have sparked significant interest in unmanned vehicles. These highly mobile robots can reach locations and perform tasks that are too difficult or even impossible for humans. As exploratory tools, they serve as platforms for onboard sensors, gathering data from previously inaccessible environments. A prime example is the ROBOVOLC project [1], which focuses on developing and testing an automated robotic system designed to explore and take measurements in volcanic areas. This robot aims to reduce the risks faced by volcanologists who work near volcanic vents during eruptions. The most critical observations and measurements of volcanic activity are often needed during the peak phases of eruptions, which unfortunately also present the greatest danger to human researchers. The robot's sensors are specifically adapted to the challenging environment, as noted in [1], and include a manipulator arm for collecting rock and gas samples, as well as deploying and retrieving instruments. It is also equipped with a pan-tilt turret, featuring a high-resolution camera, video camera, infrared camera, and a Doppler radar for measuring gas speed.

One of the most well-known examples of exploration robots is the Mars Exploration Rovers (MER), which landed on Mars in 2003, along with the earlier Pathfinder mission vehicle, Sojourner. Before Sojourner's 1997 landing on Mars, numerous stationary space probes had been sent to various planets since the 1970s. However, the mobility of Pathfinder significantly expanded the range of possible applications. The mobility of planetary rovers increased dramatically, from tens of meters with Sojourner to tens of kilometers with MER within six years. Additionally, MER showcased significant improvements in reliability, as the robots have continued to transmit valuable scientific data since 2003, over seven years after the mission's start.

Oceans have also served as a successful domain for autonomous exploration robots. In 2009, Rutgers University launched an aquatic glider, as part of [2], which became the first robot to traverse an entire ocean. The glider, named the Scarlet Knight, measured nearly eight feet in length and spent months gathering data across the Atlantic. A notable aspect of this journey was that, at times, the glider was remotely guided from locations as far away as Antarctica, utilizing satellite, GPS, and other advanced technologies.

One of the key technological advancements is the development of wireless communications, allowing systems to exchange information without physical connections. This has made it possible to replace large, complex systems with multi-agent systems that consist of multiple independent modules. In fact, utilizing a framework with multiple vehicles (whether land, marine, or aerial) can enhance efficiency, performance, flexibility, and robustness when compared to using a single, more complex vehicle. The applications of such systems span numerous fields.

In avionics, for instance, formation flight control can be applied to various tasks, such as aerial refueling or reconnaissance. A specific example, as discussed in [3], involves using multiple Unmanned

Aerial Vehicles (UAVs) for traffic monitoring, persistent surveillance, and search and rescue missions. By combining data from all the vehicles, it becomes possible to generate more accurate estimates of a target's position and velocity than would be achievable with just one vehicle.

Another area where multiple autonomous marine vehicles can make significant contributions is ocean exploration. Covering 70% of the Earth's surface, the oceans have a profound impact on the global climate and provide essential resources. To fully understand their effect on climate and oceanic biomass, more data must be gathered. Traditionally, ocean exploration has relied heavily on stationary buoys and manned surface or underwater vessels. Due to the high costs and inherent risks to human life, the number of people and vessels engaged in ocean research worldwide is relatively small. Expanding the scope of ocean exploration would require deploying a significantly larger number of vehicles. Since manned vehicles are costly, autonomous underwater and surface robots present an appealing alternative. These robots require minimal human involvement during deployment and retrieval, and their fuel and maintenance costs are far lower than those of conventional research vessels. Consequently, numerous international projects have been initiated and continue to be developed in this field.

For instance, the EU-GREX project [4] builds upon ideas presented in [5], including cooperative Autonomous Underwater Vehicle (AUV) control. This concept employs various path-following and coordination algorithms, as discussed in [6] applied to AUVs in the execution of cooperative multi-vehicle missions.

The BlueROV2 is a remotely operated vehicle (ROV) that has gained popularity for underwater exploration, inspection, and research. Built for robustness and adaptability, it can be used in various underwater scenarios such as marine research, underwater inspections, and filming. It is perfect for many underwater situations because of its compact size and manoeuvrability which allows to operate the vehicle from small boats. In its standard configuration, the BlueROV2 includes an IMU (inertial measurement unit) for navigation, a depth sensor, and a range of accessories that can be customized according to mission requirements. Optional upgrades include sonar, a manipulator arm, and advanced navigation systems, further enhancing its ability to perform detailed underwater tasks.

1.2 Objective

Despite the potential benefits, the implementation of multi-robot systems introduces new challenges, particularly in the design and execution of complex control algorithms that can effectively coordinate multiple robots. The leader-follower control strategy is one of the most widely adopted approaches for cooperative control in underwater environment. In this approach, one vehicle is designated as the leader, responsible for mission planning and trajectory control, while the other ROV function as followers, maintaining a set formation relative to the leader. This strategy simplifies the coordination of multiple

vehicles and is particularly well-suited to scenarios requiring synchronized movement and cooperation.

The integration of optical communication technology, specifically LUMA™ modems, into the leader-follower control framework, represents a significant advancement in underwater robotics. Optical communication offers several advantages over traditional acoustic methods, including higher data rates and lower latency, making it ideal for proximity and high-precision underwater operations.

In this thesis, a cooperative motion control algorithm will be developed for marine vehicles, ensuring their effectiveness by accounting for the linear dynamics of the vehicles and the challenges of underwater optical communications. The thesis specifically aims to implement a leader-follower control algorithm for a multi-robot system. In this method, the leader transmits information about its linear and angular motion - surge, sway, heave, and yaw angle to the followers through optical communication channels. Meanwhile, the follower, equipped with an onboard optical modem, uses signal strength and information received from the leader to determine its direction relative to the leader. However, due to the limitations of optical communication channels—such as limited bandwidth and minimal transmission delays—this data must be transmitted efficiently for successful coordination. This method allows for high-speed data exchange and precise control, making it an effective solution for coordinated underwater missions where traditional communication methods fall short.

1.3 Work Description

The work description for this thesis is centered around several critical tasks aimed at advancing underwater optical communication and autonomous vehicle control systems. The initial phase involved a comprehensive familiarization with the BlueROV2, supported by hands-on training sessions to understand its operational capabilities, existing control features, and technical limitations. This phase was essential for ensuring that subsequent developments aligned with the BlueROV2's functionality.

In parallel, an in-depth study of LUMA™ Optical Modems was conducted, these modems served as the primary communication link for the system. A key component of this work includes creating ROS packages for LUMA modems, which enabled streamlined communication between the modems using ROS. This integration facilitates parameter adjustments directly via the Linux terminal, allowing for real-time modifications of modem settings such as optical speed, power transmission, and number of LEDs to suit varying underwater conditions.

The evaluation and integration of LUMA™ optical modems with the BlueROV2 were major focuses, requiring careful configuration of the modems for effective underwater communication. This included testing modem performance across diverse conditions to ensure robust data exchange between the leader and follower vehicles.

The core focus of this thesis was the development and implementation of a leader-follower control

algorithm. This algorithm enables the leader vehicle to transmit its movement parameters via optical communication, allowing the follower to maintain coordinated formation and execute synchronized maneuvers. A simulation model was developed to test and refine the control algorithm under controlled conditions before deployment in real-world environments.

Finally, a comprehensive literature review on multi-agent control strategies and optical communication technologies relevant to marine vehicles supported this research. This review provides valuable insights for developing the control algorithm and grounding the thesis in the latest advancements and best practices in the field.

1.4 Contribution

This thesis significantly advances underwater robotics by integrating high-bandwidth optical communication and leader-follower control within BlueROV2 vehicles. A primary contribution is the development of custom ROS packages for LUMA™ modems, allowing direct parameter adjustments through the Linux terminal and enabling real-time adaptability in underwater communication. Additionally, the thesis introduces an optical-based leader-follower control algorithm specifically designed for low-latency, precise formation control in dynamic underwater environments. To support this development, a simulation framework was created to validate the control algorithm under controlled conditions, optimizing its performance and reducing deployment risks. Furthermore, this research provides an empirical analysis of LUMA™ modem performance across various underwater scenarios, detailing optimal deployment practices and addressing practical limitations in optical communication. Together, these contributions lay a foundation for future innovations in underwater multi-vehicle systems, particularly in exploration, environmental monitoring, and coordinated robotic missions.

1.5 Thesis Outline

This thesis is organized into five chapters, each building upon the core topics of underwater communication systems and multi-agent control for Remotely Operated Vehicles (ROVs).

- **Chapter 1: Introduction**
  The introductory chapter provides an overview of the background and motivation behind this research. It details the objectives, work carried out, and contributions made throughout the thesis.

- **Chapter 2: State of the Art**
  This chapter reviews the evolution from single-vehicle systems to multi-agent systems and the advancements in underwater communication technologies. It discusses the use of optical modems,

particularly the LUMA™ system, and highlights the associated challenges such as signal losses and hardware configurations. Additionally, it explores formation control protocols for ROVs, covering approaches like leader-follower structures, virtual structure methods, and behavior-based systems.

- **Chapter 3: Methodology**

  This chapter outlines the methods used to estimate model parameters and develop the control system. It includes discussions on mass, damping, Coriolis effects, control allocation, and reference frame transformations. The design and implementation of the leader-follower dynamics and communication protocols are discussed in detail, including the experimental platform used, such as the Robot Operating System (ROS) and the CIRTESU testing facility.

- **Chapter 4: Results and Discussions**

  The results from the experiments with optical modems and leader-follower controllers are presented and analyzed in this chapter. Key findings from the experiments are discussed, offering insights into the performance of the communication systems and control mechanisms.

- **Chapter 5: Conclusion**

  The final chapter summarizes the key outcomes of the research, outlines the contributions made, and provides recommendations for future work in the field of underwater robotic communication and control.

2

State of the Art

Contents

2.1 Evolution from one vehicle to multi-agent system

2.1.1 Advancements in Autonomous Underwater Vehicle Control

The control systems of Autonomous Underwater Vehicles (AUVs) have evolved significantly, moving from single-vehicle operations to sophisticated multi-agent systems. This evolution is largely driven by the need to handle more complex missions, improve operational efficiency, and cover larger areas of the ocean. Initially, AUV control focused on individual vehicles, where maintaining stability and precision in challenging underwater conditions was the primary goal. Early control systems, though effective in basic tasks, struggled with dynamic ocean environments due to the limitations of simplified vehicle models.

As AUV technology advanced, the introduction of adaptive and intelligent control systems marked a turning point. These systems allowed single AUVs to autonomously adapt to changing conditions such as fluctuating currents and unexpected obstacles. Neural network-based controllers [7] [8], for example, enabled AUVs to ”learn” from their surroundings and adjust their behavior in real-time, enhancing their ability to perform complex tasks. Fault-tolerant control systems [9] also emerged, ensuring that AUVs could continue their missions despite potential failures, such as thruster malfunctions. These advancements in single-vehicle control laid the foundation for the development of more complex multi-agent systems.

The transition from single-vehicle to multi-agent systems involves coordinating multiple AUVs to work together towards a common goal. Multi-agent AUV systems are essential for large-scale operations that require extensive data collection over vast areas, such as oceanographic surveys or environmental monitoring. The control strategies for these systems are far more sophisticated than those for individual vehicles. One key innovation is formation control [10], which ensures that multiple AUVs maintain a specific formation while moving through the water. This is critical in missions where the fleet’s collective behavior determines the operation’s quality and efficiency. Techniques such as Lyapunov-based control [11] and backstepping have been applied to manage and optimize formation control, allowing AUVs to remain coordinated even in the presence of environmental disturbances.

Multi-agent systems also benefit from advancements in communication technology, particularly the development of Underwater Wireless Networks (UWNs) [12]. In these systems, AUVs act as network nodes, enabling real-time communication and data exchange among vehicles. This capability allows AUVs to share information on their positions, detected obstacles, and mission progress, making it possible to coordinate complex behaviors such as synchronized movements or the division of tasks across a fleet. This level of coordination dramatically increases the efficiency and effectiveness of multi-agent AUV missions.

Leveraging the collaboration of multiple marine vehicles can significantly enhance key mission attributes such as completion time, fault tolerance, and the overall system’s perception capabilities. The

cooperation of multiple autonomous vehicles introduces substantial challenges for systems engineers, particularly in ocean exploration and monitoring, both for scientific and commercial purposes. A single vehicle's limitations, including potential system failures due to heavy equipment or inefficient data collection from covering large spatial areas, highlight the need for cooperative systems. Multiple interconnected vehicles, working in collaboration through a mobile communications network, can overcome these limitations by distributing tasks and enhancing redundancy.

Several notable research projects have demonstrated the benefits of multi-vehicle systems. For example, the MORPH project [13] successfully mapped underwater habitats using a coordinated system of one surface vehicle and four underwater vehicles, proving the advantages of fleet-based operations. Similarly, the WiMUST project [14] utilized a fleet of autonomous marine vehicles to enhance seismic data acquisition, demonstrating the replacement of conventional methods with more efficient, coordinated systems. These examples underscore the growing importance of multi-agent systems in underwater missions where precise data collection and wide area coverage are paramount.

Effective communication is essential for coordinating such multi-agent systems. Acoustic communication is the most viable method for long-range communication underwater, capable of covering thousands of meters. However, it presents challenges such as distortion from multi-path effects, long propagation delays, and limited bandwidth. To address these limitations, advances in optical communication have emerged as a complement for short-range, high-data-rate applications [15]. Although optical communication requires precise alignment between vehicles, its integration with acoustic communication enables AUVs to perform diverse tasks more efficiently.

In support of these multi-agent systems, underwater wireless sensor networks (UWSNs) have also been developed to facilitate high-bandwidth data transmission for ocean exploration. These networks consist of seabed sensors, relay buoys, AUVs, and remotely operated vehicles (ROVs), all of which work together to perform sensing, processing, and communication tasks [16]. By integrating various communication technologies, including acoustic and optical links, these networks enable real-time collaboration between vehicles, ensuring efficient data collection and environmental monitoring throughout the mission.

In conclusion, the evolution from single-vehicle control to multi-agent systems has revolutionized underwater exploration and monitoring. By leveraging advanced control techniques, robust communication networks, and cooperative vehicle strategies, multi-agent AUV systems offer a scalable and efficient solution for addressing the complex challenges of underwater missions. The integration of multiple AUVs into coordinated fleets continues to push the boundaries of what is possible in marine research, resource exploration, and environmental management.

2.1.2 Advancements in Underwater Communication for Marine Vehicles

As marine exploration expands and underwater activities increase, the demand for efficient underwater communication systems has become more critical. Traditional communication methods like acoustic waves, while useful for long-distance communication, face challenges such as limited bandwidth, high latency, and energy-intensive operation. This has led to a growing interest in Underwater Wireless Optical Communication (UWOC), which offers high bandwidth, low latency, and efficient power consumption for short-range communication. UWOC has emerged as a promising solution for real-time data transmission in underwater environments, significantly improving communication efficiency in various underwater applications, including scientific research, environmental monitoring, and resource exploration.

With the growing demands of underwater operations, such as resource extraction, wreck rescue, and the maintenance of underwater infrastructure, Autonomous Underwater Vehicles (AUVs) and Remotely Operated Vehicles (ROVs) have become integral to marine activities. These vehicles can be categorized into three main types based on their communication methods: tethered vehicles, wireless vehicles, and hybrid vehicles.

Tethered underwater vehicles are typically connected to surface control platforms via optical fibers or electrical cables [17]. These systems offer high-speed, reliable data communication and extended operational endurance. However, they are limited by their high manufacturing costs and restricted range due to the physical connection. On the other hand, wireless underwater vehicles, which communicate via acoustic waves, offer greater flexibility and can operate over vast areas. Despite this advantage, they face challenges such as limited bandwidth, long latency, and the high power consumption required by acoustic transceivers. Finally, hybrid underwater vehicles attempt to combine the advantages of both tethered and wireless systems but remain impractical for large-scale implementations due to the high costs, bulky instrumentation, and reliance on cables.

In response to these limitations, researchers have turned to Underwater Wireless Optical Communication (UWOC) to address the needs of Underwater Wireless Sensor Networks (UWSNs) for compact, durable, and high-bandwidth underwater vehicles. UWOC is particularly effective in short-distance communications, providing much higher data rates compared to acoustic methods. This has led to the integration of UWOC systems into AUVs and ROVs, enabling these vehicles to perform real-time, high-speed data transmission while reducing energy consumption.

One of the pioneering efforts in integrating UWOC into AUVs was the Autonomous Modular Optical Underwater Robot (AMOUR) [18], developed by the Computer Science and Artificial Intelligence Laboratory (CSAIL) at MIT. AMOUR was designed for underwater monitoring, exploration, and surveillance, featuring a modular design that allows it to deploy and recover sensor nodes within a network. The first iteration of AMOUR used LEDs as a light source, achieving data rates of one Kbps over a distance of two meters. This marked an important step toward enabling high-speed communication in underwater

environments.

Following the initial prototype, MIT researchers improved AMOUR by incorporating new features such as remote control, localization, and Time Division Multiple Access (TDMA), further enhancing the vehicle's capabilities. These advancements allowed AMOUR to communicate more efficiently with sensor networks and other AUVs, facilitating collaborative tasks like data transmission and cooperative navigation. In subsequent experiments, researchers demonstrated the viability of collaborative Underwater Wireless Sensor Networks (UWSNs) by utilizing AMOUR alongside other AUVs, such as the Starbug [19], to complete complex tasks. These studies validated the potential for diverse underwater vehicles to work together in a networked environment, significantly extending the operational capacity of UWSNs.

A notable enhancement came with the development of AMOUR VI, which incorporated a UWOC module for real-time control. By using blue/green LEDs as the light source, the vehicle achieved data rates in the Mbps range with latencies of just one millisecond, making it far superior to traditional acoustic communication systems, which offer data rates in the hundreds of Kbps range with significantly higher latency. The compact design of AMOUR VI, with its transmitter and receiver modules sealed in a lightweight, transparent plastic cylinder, demonstrates the feasibility of using UWOC for high-speed communication over short distances in underwater environments.

Beyond MIT's contributions, other research groups [20] [21] have developed various UWOC-enabled prototypes, further advancing the capabilities of optical wireless underwater vehicles. Some of these systems feature hybrid communication technologies, combining both acoustic and optical modules to maximize flexibility and communication efficiency. These hybrid systems offer the best of both worlds—acoustic communication for long-distance data transmission and optical communication for high-speed, short-range tasks.

In summary, the integration of UWOC into AUVs and ROVs represents a major leap forward in underwater communication technology. By enabling high-speed, low-latency data transmission, UWOC has the potential to transform underwater exploration, making it more efficient and responsive to the increasing demands of marine science, resource exploration, and environmental monitoring. As UWOC technology continues to evolve, it will play a critical role in the future of underwater wireless sensor networks and the broader field of underwater robotics.

2.1.2.A Optical Communication Link Configurations for Underwater Systems

There are four main types of Underwater Wireless Optical Communication (UWOC) configurations, classified by the nature of the links between nodes: point-to-point line-of-sight (LOS), diffused line-of-sight (DLOS), retro-reflector-based line-of-sight (RLOS), and non-line-of-sight (NLOS).

- **Point-to-Point Line-of-Sight (LOS)** In the LOS setup, a direct optical link is established between

two devices by aligning their optical transmitters and receivers. This configuration requires a clear, unobstructed path for efficient signal transmission, which is typically achieved using fixed platforms or maneuverable underwater vehicles. Point-to-point LOS offers high bandwidth, low latency, and enhanced security due to the narrow beam of the optical signal [22]. However, this method is highly dependent on environmental conditions, such as water clarity and potential obstructions from marine life, which may affect the direct view between devices

- **Diffused Line-of-Sight (DLOS)** DLOS involves the transmission of a non-directional optical signal over short to medium distances. The signal is emitted from a central source and spreads at a wide angle, allowing it to be received by multiple devices without requiring precise alignment. This configuration is beneficial for multi-point transmission and simpler setup with lower costs [23]. However, DLOS is constrained by shorter ranges, reduced data rates, high attenuation caused by seawater, multipath propagation effects, and reduced energy efficiency.

- **Retro-Reflector-Based Line-of-Sight (RLOS)** The RLOS configuration uses retro-reflectors to create an optical link between two devices. In this setup, the receiver reflects light to the transmitter, allowing for short-range, full-duplex communication. RLOS is particularly effective in scenarios where power and size constraints exist [24]. It can be optimized for photon-limited or contrast-limited environments, such as clear seawater or turbid harbor conditions. Advantages include high energy efficiency, a compact receiver, and the potential for duplex communication. However, challenges arise from signal interference due to backscatter, signal-to-noise ratio (SNR) degradation, and increased attenuation, as the signal must pass through the channel twice during transmission and reflection.

- **Non-Line-of-Sight (NLOS)** NLOS configurations are used when direct LOS between transmitter and receiver is obstructed, such as by marine life, air bubbles, or other objects. This method is ideal for short to medium-range distances where direct paths are blocked. The optical signal is reflected off surfaces like the seabed, seawater surface, or underwater objects, reaching the receiver from various angles. NLOS offers reduced requirements for precise alignment and tracking [25]. However, it faces significant challenges, including substantial signal loss, sensitivity to background radiation, and potential issues such as sea surface tilt caused by wind, which can lead to signal dispersion and reflection back to the transmitter.

2.1.2.B Technical Challenges and Performance Constraints in Underwater Optical Communication

In underwater optical communication (UWOC), the most common transmitters are laser diodes (LDs) and light-emitting diodes (LEDs), which predominantly emit light in the visible spectrum, particularly

within the blue wavelength range. However, some studies have also experimented with green and red wavelengths to enhance data transmission rates [26]. Common modulation techniques used in these systems include Pulse Amplitude Modulation 4-level (PAM4), Orthogonal Frequency Division Multiplexing (OFDM), and Quadrature Amplitude Modulation (QAM). Receivers typically use photodetectors (PDs) or avalanche photodiodes (APDs) for signal detection, with multi-pixel photon counters (MPPC) also being utilized in some cases [27]. UWOC systems can be integrated with other communication media, such as free-space optics (FSO) and plastic optical fiber (POF), broadening their application potential [28] [29].

The operational range of UWOC systems varies between studies, spanning from 2 to 100 meters. This range is heavily influenced by the type of seawater used in experiments and its specific characteristics, such as turbidity. A key performance metric for these systems is the bit error rate (BER), which measures the error frequency during data transmission and is vital for assessing communication reliability and efficiency. Data transmission rates in UWOC systems can reach gigabit-per-second (Gbps) capacities, with higher rates achievable at shorter distances (typically up to 10 meters) [30]. However, as the distance increases, the data rate tends to drop due to absorption and scattering effects. The highest recorded data rate, 500 Gbps, was achieved using PAM4 modulation, employing four channels and dual polarization techniques to boost throughput.

The ongoing development of UWOC aims to optimize data transmission over greater distances. However, it's important to note that data transmission rates and communication distances are inversely proportional—longer distances result in lower data rates. While high data rates have been achieved for short distances (1 to 10 meters), these same systems can be adapted for longer distances, albeit with reduced data rates. Even with these reductions, UWOC systems remain sufficient for certain tasks, such as establishing wireless underwater networks or controlling underwater drones [31].

2.1.2.C Optical Signal Transmission Losses

The transmission of light in underwater environments is primarily diminished by two factors: absorption and scattering. Absorption occurs when light energy is transformed into heat or other forms of energy, reducing light intensity. In marine environments, this happens when photons transfer their energy to particles within the water, decreasing the overall light output. Scattering, on the other hand, occurs when light interacts with water molecules or suspended particles, causing the light to deviate from its original path and reducing the strength of the optical signal. Both of these processes contribute to the weakening of the light signal as it travels through water. A geometric representation of the water medium, showing how absorption and scattering affect the optical signal is discussed in [32]. The corresponding geometric model is expressed with the following formula.

$$P_i(\lambda) = P_a(\lambda) + P_s(\lambda) + P_t(\lambda) \tag{2.1}$$

The incident light power is denoted by P_i, while P_a and P_s represent the fractions of the incident power that are absorbed and scattered, respectively. P_t refers to the remaining power successfully passing through the water medium. As shown in equation 2.1, the power of the light signal is influenced by its wavelength λ.

In the geometric model of the water medium, the total underwater attenuation is described by the beam extinction coefficient $c(\lambda)$, which is the sum of the absorption coefficient $a(\lambda)$ and the scattering coefficient $b(\lambda)$, as expressed in the following formula:

$$c(\lambda) = a(\lambda) + b(\lambda). \tag{2.2}$$

The absorption, scattering, and total attenuation coefficients for various marine environments are well-documented in the literature [33]. The propagation loss factor is determined by combining the total attenuation coefficient $c(\lambda)$ with the distance d, and its corresponding formula is provided below:

$$L_p(\lambda, d) = e^{-c(\lambda)d}. \tag{2.3}$$

Other factors that impact the propagation distance of an optical beam include water turbulence and the specific type of water. Variations in temperature and salinity can alter the refractive index of water, which in some cases leads to a reduction in signal propagation quality. Additionally, the composition of the water itself plays a critical role. Different types of water, which may contain varying amounts of particles, plankton, chlorophyll, and other biological matter, significantly influence the degree of absorption and scattering of light. These factors collectively shape the behavior of the optical beam and affect its transmission efficiency over distance.

Moreover, the optical properties of water vary with depth, as the marine environment is stratified into three vertical zones: the euphotic zone, dysphotic zone, and aphotic zone. The euphotic zone, located at the surface, extends up to approximately 200 meters in clear seawater and is where sunlight penetrates sufficiently for photosynthesis. Below this is the dysphotic zone, which stretches from 200 meters to several kilometers deep, receiving only faint sunlight, insufficient for photosynthesis. The aphotic zone, comprising the majority of the ocean's volume, lies beneath this layer and is characterized by complete darkness, with no sunlight penetrating this region.

2.1.3 LUMA™ Optical Modems

The LUMA X and LUMA X-UV modems [34] are advanced optical underwater communication devices designed to provide fast, reliable data transmission over significant distances. These modems operate as full transceivers, enabling half-duplex communication, meaning they can both transmit and receive data, though not simultaneously. The LUMA modems are engineered for underwater environments, where traditional radio frequency (RF) communication systems face severe limitations due to signal attenuation in water.

LUMA X modems use visible light (480 nm) for communication, while the LUMA X-UV variant operates using ultraviolet light (395 nm). Both variants are capable of transmitting data at rates ranging from 1 Mbit/s to 10 Mbit/s, depending on the optical conditions and configuration. These devices are particularly well-suited for use in environments with clear, dark water, where they can achieve communication ranges exceeding 50 meters. The modems feature software-controlled transmission power, allowing them to adjust the number of active LED banks based on the communication distance and ambient light conditions. This adaptability ensures efficient power consumption and optimal performance.

The LUMA modems can interface with both Ethernet and serial communication systems (RS232/RS485), making them versatile tools for integrating into different network configurations. Additionally, they incorporate intelligent features such as auto-speed negotiation and auto-gain control, which help to maintain stable communication even under varying environmental conditions.

These modems are compact, rugged, and rated for deepwater operations, capable of functioning at depths of up to 6000 meters, with custom configurations available for deeper deployments. Their robust design, combined with the ability to handle challenging underwater communication scenarios, makes LUMA modems ideal for applications such as underwater robotics, oceanographic research, and subsea operations where reliable wireless communication is crucial.

2.1.3.A Hardware Configuration

The physical properties of the LUMA X and LUMA X-UV modems are designed to ensure durability and functionality in underwater environments. These properties reflect the need for compactness, robustness, and resilience in challenging conditions such as high pressures, variable temperatures, and water exposure. Table 2.1 shows the key physical characteristics of the LUMA modems:

Specification	Details
Length x Diameter (Housing)	126 x 60 mm (5” x 2.4”)
Total Length with Connector	178 mm (7”)
Weight in Air	475 g (1 lb 7 oz)
Weight in Water	125 g (10.5 oz)
Connector	SubConn Ethernet Circular 8 – DBH8
Depth Rating	6000 m (19000 ft)
Operating Temperature	-5 ℃ to +40 ℃ (23 ℉ to +104 ℉)
Storage Temperature	-21 ℃ to +50 ℃ (-6 ℉ to +122 ℉)

Table 2.1: Hardware Specifications of the LUMA X Modem

The physical setup of the communication link between two LUMA X modems, as illustrated in figure 2.1, is organized to establish an optical underwater communication channel. The modems act as bridges between two separate networks, ensuring data is forwarded between the operator PC and the remote PC or server via optical signaling.

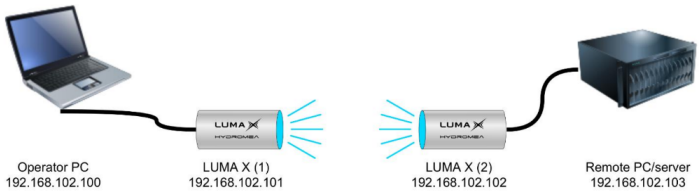

Figure 2.1: Physical Setup of LUMA Modems

Communication Flow

- The setup operates using two LUMA X modems that establish an optical communication link between the operator PC and the remote PC/server.
- LUMA X (1) receives Ethernet data from the operator PC and converts it into optical signals. These signals are transmitted through water (or a controlled environment) to LUMA X (2).
- LUMA X (2) receives the optical signals and converts them back to Ethernet data, forwarding it to the remote PC/server.
- This process allows for real-time data communication between the two PCs, using the LUMA X modems as the optical bridge.

The physical alignment of the modems is crucial, as they rely on optical signals for data transmission. Proper alignment and distance (typically at least one meter apart) ensure stable communication without signal saturation or loss. Additionally, ambient light and interference need to be minimized for optimal performance.

2.1.3.B Software Configuration

The software configuration of LUMA X modems involves a combination of using a web-based interface and an Application Programming Interface (API), both of which provide users with extensive control over the modem's operating parameters. To begin configuring the modem, users must first access the web interface by connecting the modem to a computer via an Ethernet cable. By default, each modem is assigned the IP address $192.168.102.101$, and the web interface can be accessed through a browser by entering this IP address. If multiple modems are present on the same network, the IP address of one must be changed to avoid conflicts. This can be done through the web interface by accessing the IP configuration page and setting a unique IP address, such as $192.168.102.102$.

The main configuration page of the web interface provides essential information about the modem, such as its hardware revision, firmware version, and API version. It also offers access to several configuration options that allow users to adjust key operational settings. These settings include parameters such as the auto-power feature, which automatically adjusts the modem's power level based on distance and ambient light conditions. This feature helps optimize power consumption. Additionally, the number of active LED banks, which can range from one to five, can be controlled. This setting determines how many LED banks the modem will use during transmission, with fewer LED banks reducing power consumption but potentially decreasing range.

Another critical setting is the auto-speed feature, which allows the modem to automatically adjust its optical transmission speed. If this feature is disabled, the user can manually set the speed to a value between 1 MHz and 10 MHz. Furthermore, encoding can be enabled to improve link quality, though this comes at the cost of reduced throughput. Encoding is particularly useful in environments with high optical noise, as it enhances signal stability. The auto-gain control (AGC) feature allows the modem to adapt to changes in ambient light by adjusting the receiver gain. Users can either enable AGC to automatically select sensitivity levels or manually configure the sensitivity for specific conditions.

The web interface also includes a communication test page that enables users to send test messages between two modems. This feature helps validate the communication link before proceeding with actual data transmission, ensuring the modems are correctly aligned and functioning.

In addition to the web interface, the LUMA X modems can be configured programmatically using an API based on the REST architecture. This API allows users to make HTTP requests to configure and monitor the modems. For example, users can adjust optical speed, the number of LED banks, and enable or disable auto-gain control through the API. Real-time status information, such as signal strength, temperature, and noise levels, can also be retrieved programmatically. This flexibility makes the API ideal for integrating the LUMA modems into larger systems or custom software environments where automated control is necessary.

Once configuration changes are made, they can be saved to the modem's ROM to ensure that the

settings persist after a reboot. The API also provides the option to remotely reboot the modem, which is useful for applying configuration changes or resetting the device after updates.

Firmware upgrades are another important aspect of software configuration. To upgrade the modem's firmware, users need to use the LumaConf software, which communicates with the modem via a serial connection. The modem must be put into bootloader mode for the firmware upgrade process to begin. Once in this mode, users can upload the latest firmware file and apply the update, ensuring the modem has the most current features and improvements.

Overall, the software configuration of the LUMA X modem is highly flexible and user-friendly. The combination of the web interface and API offers extensive control over the modem's performance, allowing users to adjust it to meet the needs of various underwater communication scenarios. Through these interfaces, users can optimize power usage, transmission speed, and signal quality while monitoring real-time status and applying updates when necessary.

2.1.3.C Power Configuration

The power configuration of the LUMA X modems is designed to optimize energy consumption while maintaining reliable communication performance in various underwater environments. This configuration primarily revolves around controlling the number of active LEDs, adjusting power based on signal strength and distance, and managing the modem's temperature to prevent overheating.

One of the central features in power management is the auto-power function, which allows the modem to automatically adjust its power consumption based on the distance between the two communicating modems and the level of ambient light. When enabled, the modem dynamically changes the number of active LED banks depending on the strength of the received signal. This ensures that the modem only uses the necessary amount of power for transmission, conserving energy while still maintaining a robust communication link. If the modems are far apart or if ambient light is high, more power and LED banks are used; however, when conditions are optimal (such as when the modems are close), fewer LEDs are activated, reducing power consumption.

In addition to auto-power, users can manually configure the maximum number of LED banks the modem will use during operation. The LUMA modems are equipped with up to five LED banks, and limiting the number of active banks can be an effective way to save energy. For example, if communication is taking place over a shorter distance where full power is not required, the user may set the maximum number of active LED banks to a lower value. This manual configuration allows for further control over power usage, particularly in scenarios where energy conservation is a priority.

Another key aspect of power configuration is overheat protection. When the modem operates outside of water or in situations where it begins to overheat, it automatically reduces the number of active LED banks to maintain a safe operating temperature. This ensures that the modem can continue functioning

without sustaining damage from excessive heat, particularly during extended periods of transmission or in environments where cooling is less efficient. The modem's internal systems continuously monitor temperature, and if it reaches a critical level (typically around 60° C), the modem scales back its power output by deactivating some LED banks to lower the temperature.

Power consumption is also directly related to the modem's transmission speed. Higher optical transmission speeds, such as 10 MHz, consume more energy compared to lower speeds like 1 MHz. If energy efficiency is a priority, users can configure the modems to operate at lower transmission speeds, reducing the overall power draw. This balance between speed and power allows for tailored configurations based on the specific needs of the communication environment.

In summary, the power configuration of the LUMA X modems is highly adaptable, allowing for automatic adjustments through the auto-power feature and manual control over the number of active LED banks. The modems are designed to conserve energy when possible while still delivering reliable communication, with additional protections in place to prevent overheating. These features make the LUMA modems suitable for a wide range of underwater applications, where energy efficiency and operational reliability are critical.

2.1.3.D API for Operating LUMA Modems

The LUMA modems can be operated and configured using an API (Application Programming Interface) provided by Hydromea. This API allows for communication and control of key operating parameters. The API is based on REST architecture, which means it interacts using standard HTTP requests. Table 2.2 describes the key API parameters:

API Endpoint	Parameter	Description
status.json	amplitude	Current amplitude value (auto gain selected)
	ambient	Ambient light value detected by the sensor
	temperature	Current temperature of the modem
	throughput_received_sec	Data received per second (bits/s)
	crc_errors_sec	CRC errors encountered in the last second
	pkt_recv_sec	Number of packets received per second
general_info.json	hw_version	Hardware version of the modem
	fw_version	Firmware version of the modem
	api_version	API version in use
	proc_id	Unique processor identifier
parameters.json	optical_speed	Optical speed (1, 4, 6, 8, 10 MHz)
	nb_led	Number of active LED banks (1-5)
	encoding	Encoding (0 = No encoding, 1 = Encoding)
	auto_gain_control	Automatic gain control (0 = Off, 1 = On)
	nb_receivers	Number of receivers (1-4)
	auto_power	Automatic power control (0 = Off, 1 = On)
control.json	save_parameters	Save parameters to ROM
	reset_parameters	Reset all parameters to factory defaults
	reboot	Reboot the modem
	save_ip_address	Save the IP address configuration

Table 2.2: API Parameters for Operating LUMA Modems

The LUMA modem API provides extensive control and monitoring capabilities, enabling users to adjust key parameters such as optical speed, LED banks, and gain control, as well as retrieve real-time status information. This flexibility is crucial for fine-tuning performance in various underwater environments, ensuring that the modems operate optimally under different conditions.

2.2 AUV Formation Control Protocols

The control strategies for managing formations of Autonomous Underwater Vehicles (AUVs) are generally categorized into two primary approaches: centralized coordination and decentralized coordination. In a centralized system, a central controller is responsible for planning the actions of each AUV. This controller has access to global information regarding the entire formation, allowing it to issue precise control commands that guide the collective behavior of the group. While centralized systems offer the advantage of comprehensive oversight, they tend to be less practical in dynamic underwater environments due to the reliance on constant communication and the potential for single points of failure.

On the other hand, decentralized coordination relies on the autonomy of individual AUVs. In this framework, there is no central entity directing the group's movements. Instead, each AUV operates based on locally available information and interacts with its immediate neighbors. Decentralized systems are more robust in practice, particularly in underwater environments, where communication constraints and environmental disturbances can make continuous communication difficult. AUVs in decentralized

systems are equipped with advanced sensing and decision-making capabilities, allowing them to navigate, adapt, and coordinate their actions autonomously.

Due to the self-sufficient nature of modern AUVs—capable of perceiving their surroundings, making decisions, and maintaining communication with neighboring vehicles—most research efforts have focused on developing decentralized coordination protocols. Centralized approaches, while theoretically possible, have garnered less attention in AUV/ROV formation control research, primarily because decentralized systems provide greater flexibility and robustness in real-world applications.

Given this understanding, the primary focus lies on decentralized coordination control strategies, which encompass approaches such as the leader-following structure, virtual structure, behavior-based methods, artificial potential fields, and other widely adopted frameworks.

2.2.1 Leader-Following Structure

Due to its simplicity and intuitive framework, the leader-following structure is one of the most widely used methods for controlling formations in multi-agent systems. In this approach, one or more agents are designated as leaders, while the remaining agents function as followers. Only the leaders have access to the desired reference signal, and their primary task is to track this reference trajectory. In the traditional leader-following model, there is no direct communication between the leaders and the followers. The followers' sole objective is to maintain a predetermined relative position and orientation (pose) with respect to the leaders [35] [36]. By doing so, the overall formation control goal is achieved if each vehicle reaches its target.

This method offers several advantages, including ease of implementation and flexibility in adding or removing vehicles from the formation. Furthermore, because neighboring vehicles do not interact directly, the stability of the entire formation can be analyzed using graph-based approaches, making it simpler to ensure system stability.

However, the leader-following approach has a significant drawback: the overall performance of the formation heavily depends on the behavior of the leaders and the reliability of the communication network. In underwater environments, where unpredictable faults are common, any failure of the lead agents or the communication system can potentially disrupt the entire formation. To address this vulnerability and enhance the robustness of the leader-following method, the virtual leader concept has been introduced. In this approach, no physical vehicles serve as leaders; instead, a virtual leader guides the formation, thereby mitigating the risks associated with leader or communication failures.

This method provides a more resilient solution; however, one critical challenge remains—the assumption that all vehicles in the group have access to the virtual leader's trajectory information. This is often a strong assumption and may not hold in many real-world applications, where such information may be difficult to obtain due to environmental or technical constraints.

2.2.2 Virtual Structure Approaches

The virtual structure approach is another widely used method for coordinating multi-agent formations, and it shares similarities with the virtual leader strategy. First introduced to address the cooperative control of multiple mobile robots, this approach defines a set of virtual points for each vehicle in the formation. These points are based on the desired formation configuration and the trajectory to be followed [37]. In this framework, each vehicle is assigned a specific reference point, transforming the formation-tracking problem into a position-tracking control issue. The goal is to minimize the error between the vehicle's actual position and its designated reference point. Due to its simplicity and ease of analysis, the virtual structure method has been widely adopted for achieving formation control in various applications.

However, this approach has several notable limitations. Firstly, similar to the virtual leader method, the virtual structure approach heavily depends on predefined reference trajectories, which may not always be feasible or realistic in dynamic, real-world environments. Secondly, the approach is not easily scalable; expanding the AUV formation requires redesigning the virtual reference points based on the desired formation pattern, which can be a complex and time-consuming process. Lastly, the lack of direct information exchange between neighboring vehicles limits cooperation within the formation, reducing the overall coordination performance.

2.2.3 Behavior-Based Approaches

Unlike the previously discussed methods, behavior-based approaches rely on explicit mutual communication among vehicles in a formation system. Rather than prescribing predefined reference trajectories, the behavior-based method allows each vehicle in the formation to make autonomous decisions based on locally available information, such as its state, environmental conditions, and the states of neighboring vehicles [38]. The predefined goals typically include objectives like target tracking, obstacle avoidance, collision prevention, and maintaining appropriate distances between vehicles. The control actions for each vehicle are determined by a weighted combination of these objectives, enabling the vehicle to balance multiple competing priorities.

Due to its multi-objective and distributed nature, the behavior-based approach has gained considerable attention in recent years, particularly in research related to multi-agent coordination and cooperation. Its ability to operate with only local information while still achieving global coordination makes it an attractive solution for many complex systems.

However, despite these advantages, behavior-based methods present challenges, especially when scaling the system to include more vehicles and behaviors. As the complexity of the formation grows, it becomes increasingly difficult to analyze and ensure the stability of the entire system. This limitation has

hindered the widespread practical application of behavior-based approaches in certain contexts, where the stability and predictability of the system are critical.

2.2.4 Artificial Potential Field (APF) Approaches

The Artificial Potential Field (APF) approach was originally developed by Khatib to generate obstacle-free paths for manipulators and mobile robots in path-planning tasks. The key principle of this method involves defining a set of artificial potential functions designed to guide vehicles toward their target while simultaneously avoiding obstacles. These potential functions are conceptually similar to potential energy in physics, generating corresponding forces that influence the movement of the vehicles [39]. Specifically, two types of potential functions are utilized: one generates attractive forces that pull the vehicles toward the target, and the other produces repulsive forces to push the vehicles away from obstacles, as illustrated in Figure 6. The interaction between these attractive and repulsive forces enables the vehicles to reach their goals while avoiding collisions with obstacles.

Due to its clear physical interpretation and practical applicability, the APF approach has been widely adopted in multi-agent systems to facilitate coordination and cooperation. It is particularly useful for distributed control, where vehicles rely on local information to achieve multiple objectives. Like the behavior-based approach, APF makes it relatively easy to design distributed controllers capable of achieving goals such as obstacle avoidance and target tracking without requiring global information.

Despite its strengths, the APF approach has a notable limitation: the possibility of vehicles getting trapped in points where the net force acting on them is zero, a phenomenon known as local minima. This issue can prevent the vehicles from reaching their intended targets. Additionally, as with behavior-based methods, analyzing the stability of APF-based multi-agent systems becomes increasingly complex as the size of the group grows. This complexity poses challenges in ensuring reliable performance, particularly in larger-scale applications

2.2.5 Auction-Based Approaches

Another significant strategy in multi-agent control is the auction-based approach, which focuses on dynamically allocating tasks to vehicles based on their current states and capabilities. This method is particularly effective in missions involving multiple AUVs, where each vehicle is responsible for scanning different areas or investigating specific targets. Tasks are essentially ”auctioned” to the vehicles best positioned to perform them, optimizing the overall efficiency by ensuring that each task is completed by the most capable vehicle at any given time. This strategy not only enhances resource utilization but also minimizes mission duration by allocating tasks in a way that maximizes the fleet’s effectiveness.

However, the auction-based approach is highly dependent on reliable communication between vehi-

cles, which can be problematic in underwater environments due to the challenges of transmitting data over long distances. The success of this method hinges on real-time communication to ensure that task allocation remains efficient. To mitigate communication challenges, some systems incorporate predictive models that estimate the future states of vehicles, as well as periodic synchronization, which allows coordination to be maintained even when communication is intermittent or delayed. These adaptations help ensure that the fleet continues to operate smoothly, even under suboptimal communication conditions.

2.2.6 Model Predictive Control (MPC) for AUVs

Model Predictive Control (MPC) has gained considerable attention as a method for controlling Autonomous Underwater Vehicles (AUVs) in three-dimensional space. MPC is particularly advantageous in dynamic and uncertain environments, which are common in underwater operations [40]. The strength of MPC lies in its ability to optimize control inputs in real-time by predicting the future states of both the vehicles and their surrounding environment. This predictive capability is essential for underwater missions, where variables such as water currents, obstacles, and environmental changes constantly influence vehicle behavior.

MPC operates by continuously updating control inputs based on these predictions, allowing AUVs to proactively adjust their paths to avoid hazards while maintaining coordination with other vehicles in the fleet. This dynamic adaptability ensures that AUVs can navigate efficiently, even in environments where conditions fluctuate rapidly. Moreover, MPC's real-time decision-making process enhances the overall coordination between multiple AUVs, enabling them to work together more effectively while reducing the likelihood of collisions or mission delays.

In addition to its robustness in handling uncertainties, MPC is well-suited for multi-agent systems, as it allows for distributed implementation where each AUV can independently calculate its control actions based on local information and predicted future states. This makes MPC a powerful tool for ensuring the reliability and success of complex underwater missions, especially those requiring precise navigation and coordination in challenging environments.

2.2.7 Robust H_2 Control in AUV Formation

In the context of autonomous underwater vehicles (AUVs), H_2 controllers offer a valuable approach for handling complex underwater dynamics and environmental uncertainties [41]. Using optimal control theory, H_2 controllers minimize the system's 2-norm, aligning closely with the linear quadratic Gaussian (LQG) problem and allowing for systematic robustness adjustments within feedback control systems. This optimization approach is especially relevant for AUV applications involving multi variable output

feedback, where precision in tracking and disturbance rejection is critical.

Given the underwater environment's nonlinear and coupled hydrodynamics, effective AUV control requires simplification through linearized models. By applying an H_2 control strategy to a reduced-order, linearized model of an AUV, controllers can focus on stabilizing depth-plane motion despite time delays and output disturbances. This is especially valuable for leader-follower setups, where synchronization and accurate positioning of agents are crucial. For instance, an H_2 controller enables smooth tracking of a leader vehicle by a follower even when there are model uncertainties due to environmental changes, such as varying water currents [42] [43].

Using H_2 control in AUVs helps mitigate issues like input delays, which can otherwise destabilize or reduce control accuracy. In practical tests, robust H_2 controllers demonstrate improved depth tracking and robustness over simpler controllers like PD controllers. This makes H_2 controllers well-suited for applications like underwater optical wireless communications between leader-follower AUVs, where maintaining precise alignment and communication links under dynamic conditions is essential for reliable data exchange and navigation.

As the focus shifted to multi-agent systems, the development of control strategies specifically tailored to these systems became crucial. In underwater environments, the control of multi-agent AUV systems presents unique challenges due to the harsh conditions and the limitations of underwater communication. Unlike terrestrial or aerial multi-agent systems, underwater systems must contend with the high attenuation of radio waves in water, which limits communication to low-bandwidth acoustic channels. These constraints necessitate the design of control algorithms that are robust to intermittent communication and capable of operating with minimal information exchange.

2.3 Challenges and Innovations in Underwater Communication for Multi-Agent Systems

The control of autonomous marine vehicles, particularly in multi-agent systems, has traditionally relied on various communication technologies to ensure coordination and data exchange between vehicles. Among these, acoustic communication has been the most widely adopted due to its ability to operate over long distances, sometimes reaching several kilometers. However, despite its widespread use, acoustic communication presents significant challenges that limit its effectiveness in dynamic and complex underwater environments.

One of the primary limitations of acoustic communication is its low bandwidth. Typically, acoustic channels offer data rates in the range of kilo-bits per second, which is insufficient for transmitting large amounts of data or high-frequency updates necessary for real-time control. This low bandwidth becomes a bottleneck in missions that require precise coordination between multiple vehicles, as the limited data

throughput can lead to delays in command execution and information sharing.

In addition to bandwidth limitations, acoustic communication is also plagued by high latency. The propagation speed of sound in water is much slower than electromagnetic waves in air, resulting in noticeable delays when transmitting signals over long distances. This latency can disrupt the timing of coordinated maneuvers, making it difficult to maintain formation or execute synchronized actions. Furthermore, the underwater environment introduces complexities such as multi-path distortion, where acoustic signals reflect off surfaces like the seabed or water surface, leading to interference and signal degradation. These factors contribute to a less reliable communication system, particularly in environments with complex terrain or where precision is crucial.

Radiofrequency (RF) communication, while commonly used in terrestrial and aerial applications, faces severe limitations underwater. The high attenuation of RF signals in water restricts their effective range to just a few meters, rendering RF communication impractical for long-distance interactions between underwater vehicles. Even within its short range, RF communication demands significant power to penetrate the water medium, which is a considerable drawback given the energy constraints typically faced by autonomous vehicles. The combination of short-range and high energy consumption makes RF communication less suitable for coordinating multiple AUVs in a marine environment, particularly when those vehicles need to operate over large areas.

Hybrid communication systems, which attempt to combine the strengths of acoustic and optical or RF communication, have been proposed to address some of these limitations. These systems aim to use acoustic signals for long-range communication while leveraging optical or RF signals for high-bandwidth, short-range exchanges. However, these hybrid approaches introduce new challenges. The management of multiple communication channels increases the system's complexity and may introduce additional points of failure. Moreover, hybrid systems are still subject to the inherent limitations of the individual communication technologies they incorporate. For instance, while optical communication offers high data rates, it requires line-of-sight between vehicles and is limited in range, making it difficult to maintain consistent communication in environments where the vehicles may be separated by obstacles or varying terrain.

2.3.1 Leader-Follower Controller Using LUMA ™ Optical Modems: A State-of-the-Art Approach

In contrast to the aforementioned methods, the leader-follower control algorithm implemented using optical communication represents a significant advancement in the field of underwater vehicle coordination. This approach addresses many of the challenges posed by traditional communication methods by leveraging the strengths of optical communication within a well-defined control framework.

Optical communication, unlike acoustic or RF methods, offers significantly higher data rates, reach-

ing into the megabits per second range. This capability is particularly advantageous in scenarios where vehicles need to exchange large amounts of data rapidly, such as during complex coordinated maneuvers or when sharing sensor data in real time. The leader-follower control strategy enhances this by simplifying the communication requirements. In this setup, one vehicle—the leader—takes on the responsibility of navigation and path planning, while the follower vehicle maintains a set formation relative to the leader. This reduces the need for continuous, bidirectional communication and allows the follower to rely on periodic updates from the leader, ensuring that both vehicles stay coordinated.

The primary limitation of optical communication is its requirement for line-of-sight and its limited range. However, these limitations are mitigated in the leader-follower configuration, where the vehicles are kept close, ensuring a stable optical link. By focusing on short-range, high-bandwidth communication, the system maximizes the benefits of optical communication while avoiding the pitfalls of long-range acoustic communication's low bandwidth and high latency. This makes the leader-follower approach not only effective but also highly reliable, as it reduces the likelihood of communication interruptions and ensures that the follower vehicle can respond promptly to the leader's commands.

In the event of a temporary loss of communication, the follower vehicle is programmed to use signal strength as a backup mechanism. By interpreting signal strength indicators, the follower can locate the leader's approximate position and re-establish communication. When communication is lost, the follower switches to a search mode using signal strength as a feedback parameter. It initiates a systematic scanning maneuver, such as spiraling or moving in a grid pattern, while continuously monitoring the signal strength of any intermittent optical signal detected. The objective is to maximize signal strength, guiding the follower closer to the leader. Once optimal signal strength is re-established, indicating that the leader is within effective communication range, the follower attempts to reinitiate full communication. Additionally, the follower vehicle will send an automatic alarm to the remote operator, notifying them of the communication loss, and enabling further intervention if needed.

The simplicity of the leader-follower model contributes to the robustness of the system. The follower vehicle mirrors the leader's actions, following its path and maintaining the desired formation. This reduces the computational burden on the follower and minimizes the potential for errors, as the system's success hinges on the performance of the leader vehicle, which can be equipped with more sophisticated navigation and control systems.

In summary, the leader-follower control algorithm using optical communication is a state-of-the-art solution that effectively addresses the challenges of underwater vehicle coordination. By leveraging optical communication's high data rates and the straightforward nature of the leader-follower dynamic, this approach offers a robust, reliable, and efficient method for managing two marine vehicles in coordination. The strategic use of optical communication within this framework not only improves the precision of coordinated actions but also enhances the system's overall reliability, making it a superior choice

compared to traditional methods.

3

Methodology

Contents

This part of this chapter will focus on the SNAME [44] (Society of Naval Architects and Marine Engineers) notation for marine craft, diving into a standard framework used to describe and categorize the physical and operational characteristics of marine vehicles, including ROVs like the BlueRov2. The notation of marine vehicles are summarised for all 6 degrees of freedom in the tables 3.1 and 3.2:

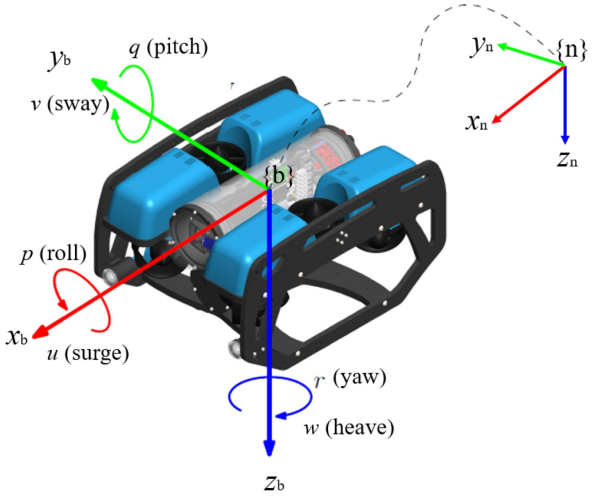

Figure 3.1: BlueROV 2

DOF	Forces/Moments	Linear &Angular Velocities	Positions/Angles(euler)
Surge	X	u	x
Sway	Y	v	y
Heave	Z	w	z
Roll	K	p	ϕ
Pitch	M	q	θ
Yaw	N	r	ψ

Table 3.1: SNAME notation for Marine Vessels

DOF	Added Mass	Linear Damping
Surge	$X_{\dot{u}}$	X_u
Sway	$Y_{\dot{v}}$	Y_v
Heave	$Z_{\dot{w}}$	Z_w
Roll	$K_{\dot{p}}$	K_p
Pitch	$M_{\dot{q}}$	M_q
Yaw	$N_{\dot{r}}$	N_r

Table 3.2: SNAME notation for hydrodynamic parameters.

3.1 Estimation of Model Parameters

The dynamic equations of motion for an ROV, drawn from Fossen's vectorial robot model [41], consist of the kinematic equation 3.1 and the kinetic equation 3.2, outlined below:

$$\dot{\eta} = J(\eta)\upsilon \tag{3.1}$$

$$M\dot{\upsilon} + C(\upsilon)\upsilon + D(\upsilon)\upsilon + g(\eta) = \tau \tag{3.2}$$

where

$$\eta = \begin{bmatrix} x \\ y \\ z \\ \psi \end{bmatrix}; \upsilon = \begin{bmatrix} u \\ v \\ w \\ r \end{bmatrix} \tag{3.3}$$

The equation (3.1) gives the relationship between the velocities in the body frame and NED frame, where J is the transformation matrix between the body and the NED frame. The equation (3.2) is in the body frame and is divided into rigid body forces and hydrodynamic forces.

- M = $M_{RB} + M_A$ is the mass matrix that contains the rigid body mass and added mass effects.
- C = $C_{RB} + C_A$ is the coriolis force due to rigid body and added mass effects.
- D = $D_L + D_{NL}$ is the linear and non-linear damping forces.
- η is the position and orientation in NED frame, and ν is the velocities in body frame.
- g is the force due to gravity and buoyancy affecting the marine system.
- g_0 is an optional term that is the static restoring forces and moments due to ballast systems and water tanks.
- τ is the combination of outside forces acting on the system which includes the force from thrusters control, current etc.

For this thesis work, control is implemented with four degrees of freedom: surge, sway, heave, and yaw. It is assumed that the BlueROV2 has been designed with inherent stability in the pitch and roll axes, eliminating the need for active control in these degrees of freedom. The scope of this work focuses on low-speed operations, where certain dynamic effects, such as Coriolis forces and added mass in specific directions, can be considered negligible. This allows for simplifications in the system dynamics, reducing the computational load and improving the efficiency of the control algorithms. The estimation and measurement methods for each critical parameter will be discussed in detail, along with the justification for

neglecting specific parameters that have minimal influence on system behavior at the operating speeds considered.

3.1.1 Mass and Added Mass

The mass matrix consists of the rigid body mass and the added mass

$$M := M_{RB} + M_A \tag{3.4}$$

For the reduced 4DoF model, these are considered as in [41], as

$$\begin{aligned} M_{RB} &:= \begin{bmatrix} m & 0 & 0 & 0 \\ 0 & m & 0 & 0 \\ 0 & 0 & m & 0 \\ 0 & 0 & 0 & I_z \end{bmatrix} \\ M_A &:= \begin{bmatrix} -X_{\dot{u}} & 0 & -X_{\dot{w}} & 0 \\ 0 & -Y_{\dot{v}} & 0 & mx_g - Y_{\dot{r}} \\ -X_{\dot{w}} & 0 & -Z_{\dot{w}} & 0 \\ 0 & mx_g - Y_{\dot{r}} & 0 & -N_{\dot{r}} \end{bmatrix}, \end{aligned} \tag{3.5}$$

where $X_{\dot{u}}, Y_{\dot{v}}, Z_{\dot{w}}$ are the added mass coefficients in the surge, sway, and heave directions, respectively. $N_{\dot{r}}$ is the added mass coefficients related to the yaw motion. m is the mass of the BlueROV2 and $x_g = 0$. These coefficients represent the additional inertia that needs to be overcome due to the acceleration of water as the vehicle moves. They are crucial for accurately modeling and controlling the dynamics of underwater vehicles. In practical applications, the off-diagonal elements of M_A are often negligible compared to the diagonal terms. As a result, the added mass matrix can be simplified to:

$$M_A = M_A^\top = - \begin{bmatrix} X_{\dot{u}} & 0 & 0 & 0 \\ 0 & Y_{\dot{v}} & 0 & 0 \\ 0 & 0 & Z_{\dot{w}} & 0 \\ 0 & 0 & 0 & N_{\dot{r}} \end{bmatrix}$$

These hydrodynamic parameters of added mass are taken from [45]

$$M_A = - \begin{bmatrix} 5.5 & 0 & 0 & 0 \\ 0 & 12.7 & 0 & 0 \\ 0 & 0 & 14.57 & 0 \\ 0 & 0 & 0 & 0.12 \end{bmatrix}$$

Each coefficient quantifies the additional inertia that must be overcome due to the acceleration of water in each respective motion direction. This matrix is crucial for accurately modeling the dynamic behavior of underwater vehicles in these considered four degrees of freedom.

3.1.2 Damping Loads

The damping forces can be divided into linear and nonlinear forces according to [41], given as

$$D(\nu_r) := D_L + D_{NL}(\nu_r), \tag{3.6}$$

where

$$D_L := \begin{bmatrix} X_u & 0 & 0 & 0 \\ 0 & Y_v & 0 & 0 \\ 0 & 0 & Z_w & 0 \\ 0 & 0 & 0 & N_r \end{bmatrix} \tag{3.7}$$

$$D_{NL} := \begin{bmatrix} X_{|u|u}|u| + X_{uuu}u^2 & 0 & 0 & 0 \\ 0 & Y_{|v|v}|v| + Y_{vvv}v^2 & 0 & 0 \\ 0 & 0 & Z_{|w|w}|w| + X_{www}w^2 & 0 \\ 0 & 0 & 0 & N_{|r|r}|r| + N_{rrr}r^2 \end{bmatrix}. \tag{3.8}$$

In this thesis work, the nonlinear damping terms will be omitted since, at low speeds, the linear terms have a more significant influence.

The parameters for the linear terms will be determined through an experimental setup, which will be used to identify the lateral damping forces as proposed by [46]. It is assumed that the damping coefficients remain consistent across operations. Consequently, the damping coefficients and the corresponding damping matrix are determined as follows:

$$D_L := \begin{bmatrix} -4.03 & 0 & 0 & 0 \\ 0 & -6.22 & 0 & 0 \\ 0 & 0 & -5.18 & 0 \\ 0 & 0 & 0 & -0.07 \end{bmatrix} \tag{3.9}$$

3.1.3 Coriolis Effects

The Coriolis-centripetal matrix is a combination of the rigid body and the added mass effects, given as

$$C(\nu) := C_{RB}(\nu) + C_A(\nu). \tag{3.10}$$

For rigid body in 6DOF, $C_{RB}(\nu)$ is given as

$$C_{RB}(\nu) = \begin{bmatrix} 0 & -mS(\nu_1) - mS(\nu_2)S(r_g^b) \\ -mS(\nu_1) + mS(r_g^b)S(\nu_2) & S(I_b\nu_2) \end{bmatrix}, \tag{3.11}$$

where m is the mass, I_b is the inertia matrix about CO, S is the cross-product operator, r_g^b is the distance vector from CO to CG, and $\nu_1 = [u, v, w]^T$ and $\nu_2 = [p, q, r]^T$ [41]. The CO is taken to be CG, which means that $r_g^b = 0$. This reduces to

$$C_{RB}(\nu) = \begin{bmatrix} 0 & 0 & 0 & mv \\ 0 & 0 & 0 & -mu \\ 0 & 0 & 0 & 0 \\ mv & -mu & 0 & 0 \end{bmatrix}, \tag{3.12}$$

while the coriolis-added matrix is modelled as

$$C_A(\nu_r) = \begin{bmatrix} 0 & 0 & 0 & Y_{\dot{v}}v \\ 0 & 0 & 0 & -X_{\dot{u}}u \\ 0 & 0 & 0 & 0 \\ -Y_{\dot{v}}v & X_{\dot{u}}u & 0 & 0 \end{bmatrix}. \tag{3.13}$$

3.1.4 Control Allocation

The control forces acting on the ROV, denoted by τ, describe the relationship between the thruster forces and the resulting loads on the ROV. The 4DOF control forces for surge, sway, heave, and yaw are expressed in body coordinates as:

$$\tau := \begin{bmatrix} F_x \\ F_y \\ F_z \\ M_z \end{bmatrix} \tag{3.14}$$

For this thesis, a thrust allocation matrix that translates the thruster forces into the corresponding 4DOF body forces was already computed [45]. As a result, only the body control loads F_x, F_y, F_z, M_z will be used directly.

3.1.5 Transformation between reference frames

The transformation matrix, which is the combination of the rotation and translation matrix according to [41] is given as

$$J_\Theta(\eta) := \begin{bmatrix} R(\Theta)_{nb} & 0_{3\times3} \\ 0_{3\times3} & T(\Theta)_{nb} \end{bmatrix}, \tag{3.15}$$

and the reduced 4DoF matrix is

$$J = \begin{bmatrix} \cos\psi & -\sin\psi & 0 & 0 \\ \sin\psi & \cos\psi & 0 & 0 \\ 0 & 0 & 1 & 0 \\ 0 & 0 & 0 & 1 \end{bmatrix}. \tag{3.16}$$

This matrix is used in the conversion from the NED frame to the Body frame.

3.2 Control System Design

The development of distributed protocols for networked multi-agent systems has been a prominent research area in systems and control over the past two decades. This interest stems from the wide range of potential applications for multi-agent systems, including smart grids, formation control, and intelligent transportation systems. A key challenge in linear multi-agent systems lies in designing distributed protocols that minimize given quadratic cost functions while ensuring that the agents achieve a common objective, such as synchronization.

This thesis work addresses the distributed H_2 optimal control problem for multi-agent systems using dynamic output feedback. Specifically, it examines a system with one leader and one follower, aiming to develop a protocol that guarantees consensus between the two agents, while maintaining the H_2 cost below a predetermined upper limit. Communication between the leader and follower is facilitated through LUMA™ optical modems, which transmit the leader's states.

3.2.1 Notations

In this work, the set of real numbers is represented by $\mathbb{R}$, and the space of n-dimensional real vectors is denoted as $\mathbb{R}^n$. The vector $\mathbf{1}_n \in \mathbb{R}^n$ has all its components equal to 1, and I_n represents the identity matrix of size $n \times n$. For a symmetric matrix P, we write $P > 0$ if P is positive definite, and $P < 0$ if P is negative definite. The trace of a square matrix A is denoted as tr(A). A matrix is considered Hurwitz if all of its eigenvalues have negative real parts. The diagonal matrix with elements $d_1, d_2, \ldots, d_n$ on its diagonal is denoted by diag$(d_1, d_2, \ldots, d_n)$, where $d_1, d_2, \ldots, d_n$ are scalars. For a set of matrices $M_1, M_2, \ldots, M_m$, the block diagonal matrix with diagonal blocks M_i is written as blockdiag$(M_1, M_2, \ldots, M_m)$. The Kronecker product of two matrices A and B is denoted by $A \otimes B$.

3.2.2 Graph Theory

A directed weighted graph is denoted by $(\mathcal{V}, \mathcal{E})$, where $\mathcal{V} = \{1, 2, \ldots, N\}$ represents the set of nodes, and $\mathcal{E} = \{e_1, e_2, \ldots, e_M\}$ represents the set of edges, such that $\mathcal{E} \subseteq \mathcal{V} \times \mathcal{V}$. The adjacency matrix $\mathcal{A} = [a_{ij}]$ consists of non-negative elements a_{ij}, which represent the edge weights. If $(i, j) \in \mathcal{E}$, then $a_{ji} > 0$; otherwise, $a_{ji} = 0$.In the given graph theory context, the indices i and j represent the nodes of the graph. The pair $(i, j) \in \mathcal{E}$ represents an edge from node i to node j, where $\mathcal{E}$ is the set of edges. If the graph is undirected, $(i, j) \in \mathcal{E}$ implies $(j, i) \in \mathcal{E}$, meaning the edge is bidirectional between nodes i and j. If $i = j$, it represents a loop, which is not allowed in a simple graph, as $(i, i) \notin \mathcal{E}$.

A graph is undirected if $a_{ij} = a_{ji}$ for all i, j. It is referred to as simple if $a_{ii} = 0$ for all i. A simple undirected graph is connected if, for each pair of nodes i and j, there is a path from i to j. For a given

simple undirected weighted graph $\mathcal{G}$, the degree matrix is the diagonal matrix $\mathcal{D} = \text{diag}(d_1, d_2, \ldots, d_N)$, where $d_i = \sum_{j=1}^{N} a_{ij}$. The Laplacian matrix of the graph is defined as $L = \mathcal{D} - \mathcal{A}$.

For an undirected graph, the Laplacian matrix is symmetric, and its eigenvalues are non-negative. A simple undirected graph is connected if and only if the Laplacian matrix has a simple eigenvalue at zero. In this case, there exists an orthogonal matrix U such that $U^\top L U = \Lambda = \text{diag}(0, \lambda_2, \ldots, \lambda_N)$, with $0 < \lambda_2 \leq \cdots \leq \lambda_N$.

3.2.3 Leader-Follower Dynamics

We consider a leader-follower network, where the underlying graph consists of one leader (indexed as l) and one follower (indexed as i). The dynamics of both agents are described by the nominal finite-dimensional linear time-invariant system.

The leader's dynamics are described as:

$$\begin{aligned} \dot{x}_l(t) &= Ax_l(t), \\ y_l(t) &= C_1 x_l(t), \\ z_l(t) &= C_2 x_l(t) \end{aligned} \tag{3.17}$$

while the follower's dynamics are given by:

$$\begin{aligned} \dot{x}_i(t) &= Ax_i(t) + Bu_i(t) + Ed_i(t), \\ y_i(t) &= C_1 x_i(t) + D_1 d_i(t), \\ z_i(t) &= C_2 x_i(t) + D_2 u_i(t) \end{aligned} \tag{3.18}$$

where x_i, y_i, z_i, u_i, d_i represent the state, measured output, output to be controlled, input, and external disturbance for the follower, respectively. The matrices $A, B, C_1, C_2, D_1, D_2, E$ have appropriate dimensions. We assume that the pair (A, B) is controllable and (C_1, A) is observable. Both agents follow the same linear input-output model.

It is assumed that the follower has access to the relative output measurements from the leader, and we use output feedback protocols. Following the approach in [47], the observer-based distributed dynamic protocol is:

$$\begin{aligned} \dot{w}_i &= (A - GC_1)w_i + \sum_{j \in \mathcal{N}_i} [BF(w_i - w_j) + G(y_i - y_j)], \\ u_i &= Fw_i \end{aligned} \tag{3.19}$$

where $G \in \mathbb{R}^{n \times r}$ and $F \in \mathbb{R}^{m \times n}$ are feedback gain matrices designed to ensure synchronization between the leader and the follower. The leader's state is available to the follower through a simple, undirected, and connected graph. To understand the structure of this protocol, notice that agent i re-

ceives information $\sum_{j\in\mathcal{N}_i}(y_i - y_j)$, i.e., the sum of the relative outputs with respect to its neighbors. The first equation has the structure of an observer for the sum of the relative states, i.e., $\sum_{j\in\mathcal{N}_i}(x_i - x_j)$, with w_i representing the estimated value. It can be easily seen that the error $e_i := w_i - \sum_{j\in\mathcal{N}_i}(x_i - x_j)$ satisfies the dynamics

$$\dot{e}_i = (A - GC)e_i. \tag{3.20}$$

The second equation is a static gain, feeding the estimate w_i back to agent i. By interconnecting the agents using this protocol, we obtain the closed-loop dynamics of the entire network as:

$$\begin{aligned} \dot{\mathbf{x}} &= (I \otimes A)\mathbf{x} + (I \otimes B)\mathbf{u} + (I \otimes E)\mathbf{d}, \\ \mathbf{y} &= (I \otimes C_1)\mathbf{x} + (I \otimes D_1)\mathbf{d} \end{aligned} \tag{3.21}$$

and,

$$\begin{aligned} \dot{\mathbf{w}} &= \left[(I \otimes (A - GC_1)) + (L \otimes BF)\right]\mathbf{w} + (L \otimes G)\mathbf{y}, \\ \mathbf{u} &= (I \otimes F)\mathbf{w}. \end{aligned} \tag{3.22}$$

This leads to the network dynamics:

$$\begin{bmatrix} \dot{\mathbf{x}} \\ \dot{\mathbf{w}} \end{bmatrix} = \begin{bmatrix} I \otimes A & I \otimes BF \\ L \otimes GC_1 & I \otimes (A - GC_1) + (L \otimes BF) \end{bmatrix} \begin{bmatrix} \mathbf{x} \\ \mathbf{w} \end{bmatrix} + \begin{bmatrix} I \otimes E \\ L \otimes GD_1 \end{bmatrix} \mathbf{d} \tag{3.23}$$

Primarily, we aim for the protocol 3.19 to solve the leader-follower consensus control issue for agents 3.17 and 3.18. In the leader-follower consensus framework, the followers' states must match the leader's state. Thus, we are concerned with the differences between the states of the leader and followers. To formalize this, we introduce the error state variable for the follower as $e_i = x_i - x_l$, where the leader-follower consensus is achieved if $e_i = 0$, as $t \to \infty$.

In the case of distributed H_2 optimal control for multi-agent systems, we focus on the differences between the leader's and followers' output values. Thus, the performance output variable is $\epsilon_i = z_i - z_l$, representing the output disagreement between the leader and the followers.

The dynamics of this error system yield the following controlled error system:

$$\begin{bmatrix} \dot{\mathbf{e}} \\ \dot{\mathbf{w}} \end{bmatrix} = \begin{bmatrix} I \otimes A & I \otimes BF \\ L \otimes GC_1 & I \otimes (A - GC_1) + (L \otimes BF) \end{bmatrix} \begin{bmatrix} \mathbf{e} \\ \mathbf{w} \end{bmatrix} + \begin{bmatrix} I \otimes E \\ L \otimes GD_1 \end{bmatrix} \mathbf{d} \tag{3.24}$$

and,

$$\epsilon = \begin{bmatrix} I_{N-1} \otimes C_2 & I_{N-1} \otimes D_2F \end{bmatrix} \begin{bmatrix} \mathbf{e} \\ \mathbf{w} \end{bmatrix}. \tag{3.25}$$

Simplifying 3.24 and 3.25 gives us:

$$\begin{bmatrix} \dot{\mathbf{e}} \\ \dot{\mathbf{w}} \end{bmatrix} = \begin{bmatrix} A_w \end{bmatrix} \begin{bmatrix} \mathbf{e} \\ \mathbf{w} \end{bmatrix} + \begin{bmatrix} B_w \end{bmatrix} \mathbf{d} \tag{3.26}$$

and,

$$\epsilon = \begin{bmatrix} C_w \end{bmatrix} \begin{bmatrix} \mathbf{e} \\ \mathbf{w} \end{bmatrix}. \tag{3.27}$$

The impulse response matrix of this controlled error system is:

$$h_{F,G}(t) = C_w e^{tA_w} B_w \tag{3.28}$$

Associated cost function H_2 derived from [48] is:

$$J(F,G) := \int_0^\infty \text{tr}\left[h_{F,G}^\top(t) h_{F,G}(t)\right] dt. \tag{3.29}$$

The network is considered synchronized by the protocol if, we have $x_f \to x_l$ and $w_i \to 0$ as $t \to \infty$. For an undirected graph, the Laplacian L is a real symmetric matrix, so there exists an orthogonal $p \times p$ matrix U that transforms L into the diagonal form $U^\top L U = \Lambda := \text{diag}(0, \lambda_2, \lambda_3, \ldots, \lambda_p)$. Additionally, we assume the graph is connected, which implies $\lambda_2 > 0$. By applying the state transformation.
The network equation then becomes:

$$\begin{bmatrix} \dot{\check{\mathbf{e}}} \\ \dot{\check{\mathbf{w}}} \end{bmatrix} = \begin{bmatrix} I \otimes A & I \otimes BF \\ \Lambda \otimes GC & I \otimes (A - GC_1) + (\Lambda \otimes BF) \end{bmatrix} \begin{bmatrix} \check{\mathbf{e}} \\ \check{\mathbf{w}} \end{bmatrix}. \tag{3.30}$$

An auxiliary dynamic system is introduced with the associated dynamic feedback controller as:

$$\begin{aligned} \dot{\tilde{e}}_i(t) &= A\tilde{e}_i(t) + B\tilde{u}_i(t) + E\tilde{d}_i(t), \\ \tilde{\xi}_i(t) &= C_1\tilde{e}_i(t) + D_1\tilde{d}_i(t), \\ \tilde{\epsilon}_i(t) &= C_2\tilde{e}_i(t) + D_2\tilde{u}_i(t), \end{aligned} \tag{3.31}$$

where $\tilde{e}_i \in \mathbb{R}^n$, $\tilde{u}_i \in \mathbb{R}^m$, $\tilde{d}_i \in \mathbb{R}^q$, $\tilde{\xi}_i \in \mathbb{R}^r$, and $\tilde{\epsilon}_i \in \mathbb{R}^p$ are the state, coupling input, external disturbance, measured output, and the output to be controlled of the ith auxiliary system. By using the associated dynamic feedback controllers:

$$\dot{\tilde{w}}_i = A\tilde{w}_i + B\tilde{u}_i + G(\tilde{\xi}_i - C_1\tilde{w}_i), \tilde{u}_i = \lambda_i F\tilde{w}_i \tag{3.32}$$

The closed-loop system can be written as:

$$\begin{bmatrix} \tilde{e}_i \\ \tilde{w}_i \end{bmatrix} = \begin{bmatrix} A & \lambda_i BF \\ GC_1 & A - GC_1 + \lambda_i BF \end{bmatrix} \begin{bmatrix} \tilde{e}_i \\ \tilde{w}_i \end{bmatrix} + \begin{bmatrix} E \\ GD_1 \end{bmatrix} \tilde{d}_i, \tag{3.33}$$

$$\epsilon_i = \begin{bmatrix} C_2 & \lambda_i D_2 F \end{bmatrix} \begin{bmatrix} \tilde{e}_i \\ \tilde{w}_i \end{bmatrix} \tag{3.34}$$

The goal is to design local feedback gain matrices $G \in \mathbb{R}^{n \times r}$ and $F \in \mathbb{R}^{m \times n}$, given $\gamma > 0$, such that the

dynamic protocol 3.19 achieves leader-follower consensus and satisfies $J(F,G) < \gamma$.

To internally stabilize the controller 3.32, the following condition should be set to true: $D_1 E^\top = 0$, $D_2 C_2 = 0$, $D_1 D_1^\top = I_r$, and $D_2^\top D_2 = I_m$. These can be substituted by the regularity conditions $D_1 D_1^\top > 0$ and $D_2^\top D_2 > 0$ alone. [48] provides sufficient conditions to derive the gain matrices F and G, to synchronize the network and to ensure suboptimality, i.e., $J(F,G) < \gamma$. In fact, G is chosen as $QC_1^\top$, where $Q > 0$ is a solution to the Riccati inequality:

$$AQ + QA^\top - QC_1^\top C_1 Q + EE^\top < 0. \tag{3.35}$$

Let there be a *c* such that $0 < c < \frac{2}{\lambda_i^2}$.
where λ_i is the eigenvalue of L, then there exists $P > 0$ such that

$$A^\top P + PA + (c^2\lambda_i^2 - 2c\lambda_i) PBB^\top P + C_2^\top C_2 < 0. \tag{3.36}$$

If P and Q also satisfy

$$\text{tr}(C_1 QPQC_1^\top) + \text{tr}(C_2 QC_2^\top) < \gamma, \tag{3.37}$$

then the protocol 3.19 with $F := -cB^\top P$ and $G := QC_1^\top$ ensures leader-follower consensus for agents 3.17 and 3.18, and the protocol is sub-optimal, i.e., $J(F,G) < \gamma$.
The states of the leader are sent to the follower using the LUMA™ optical modems.

3.3 Communication Link

In this setup, the communication link between two modems is established using the LUMA™ optical modems. The two LUMA modems, one installed on each marine vehicle, are configured to communicate with each other, facilitating data transfer between the vehicles. The communication tool is employed to create and assess the link between the two modems, ensuring reliable and efficient communication.

One of the modems is designated as the server, while the other operates as the client. The server modem passively waits to receive data, while the client initiates the communication by sending the information about its pose to the server. This setup also allows the measurement of network performance parameters such as bandwidth, signal strength, and data transfer rates between the modems, which is essential for ensuring the quality and reliability of the communication link.

Additionally, this communication system is integrated into a ROS Noetic environment, which manages the data exchanged between the two marine vehicles. The ROS nodes control the system's operations, while Rosbag records data logs, enabling post-mission analysis of communication performance. The system is capable of monitoring the quality of the communication link, ensuring robust and stable data transmission between the modems, even in challenging underwater conditions. This ensures

seamless coordination between the two vehicles during mission-critical tasks.

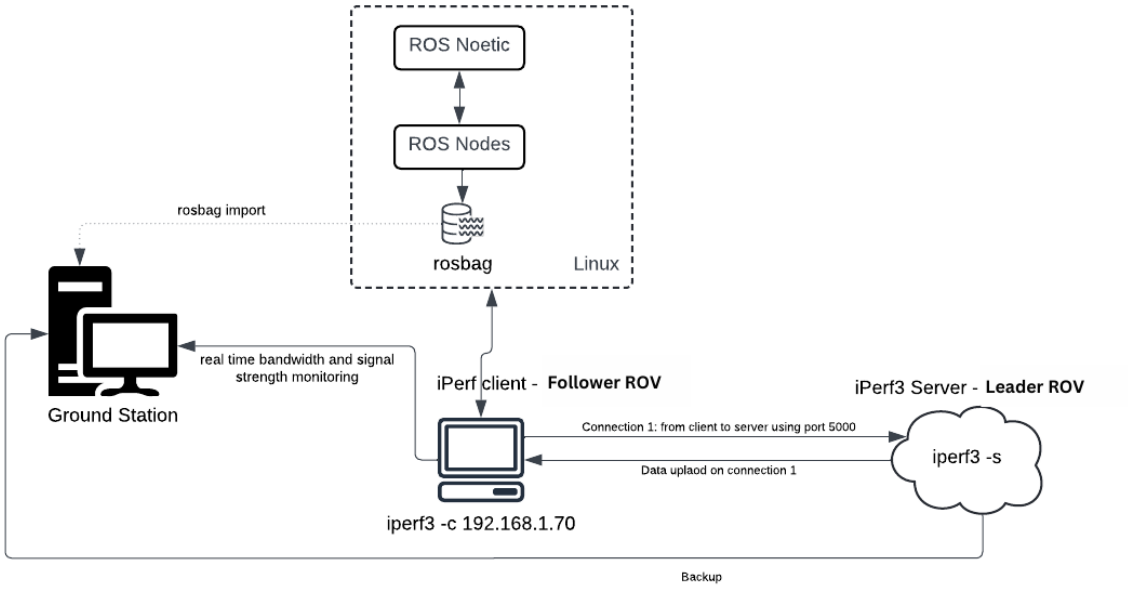

Figure 3.2: Communication Protocol

3.4 Experimental Platform

3.4.1 Robot Operating System (ROS)

Robot Operating System (ROS) [49] is a versatile framework designed for developing robot software. It provides a set of guidelines, libraries, and tools aimed at simplifying the creation of advanced and reliable robotic behavior across various platforms. Due to its extensive library, strong community support, and flexibility, ROS is widely adopted for numerous robotic applications. In this thesis work, ROS 1 has been utilized to integrate the modems and execute different functionalities, specifically using the Noetic version of ROS 1.

ROS 1 is based on the concept of nodes, which are individual processes responsible for computation. A typical robotics system comprises several nodes, with communication between them achieved through message passing. These messages can be simple, such as numbers, or more complex, like a 3D pose.

Communication in ROS 1 takes place over topics, where one node publishes information to a topic, and another node subscribes to that topic to receive the data. Additionally, ROS 1 offers services, which enable synchronous remote procedure calls, allowing a node to send a request and await a response. The ROS Master acts as a name server, managing the registration and discovery of nodes within the

system. ROS also includes a logging feature called 'bags' that allows for the recording and playback of message data within the system.

3.4.1.A LUMA™ ROS Package

The LUMA ROS package was created to facilitate the control and configuration of the LUMA X modem through the ROS (Robot Operating System) interface. While LUMA already offers a web-based interface to modify key operating parameters, this package enables the modification of these parameters via the ROS terminal, using Python programming. The LUMA X modem can be configured and monitored using the API provided by Hydromea, which adheres to the REST architecture. This means the modem can interact using standard HTTP requests. Using Python's requests library, the LUMA ROS package includes a ROS node that communicates directly with the LUMA modem, allowing parameter modifications without requiring the web interface.

To integrate the LUMA modem into a ROS environment, the Python requests commands were encapsulated into ROS services and action clients. This allows ROS users to control and monitor the modem parameters using ROS messages and services. For example, the *luma_parameter*s service provides an interface to adjust parameters like optical speed or LED configuration directly from the ROS terminal.

The key API parameters are described in Table 2.2. This table outlines the various modifiable parameters, including optical_speed, nb_led, and auto_gain_control, along with endpoints like status.json and parameters.json which facilitate data monitoring and configuration.

This integration not only simplifies the operational workflow but also allows the LUMA modem to be seamlessly integrated into larger underwater robotic systems managed by ROS. By using the ROS framework, the LUMA modem parameters can be dynamically adjusted in response to environmental conditions or mission requirements, improving flexibility and overall system efficiency.

3.4.2 CIRTESU (Centre for Research in Robotics and Underwater Technologies

The CIRTESU at Universitat Jaume-I (UJI), Spain, was used to perform several tests with the optical modems. CIRTESU is a cutting-edge facility dedicated to research and testing in robotics and underwater technologies. This laboratory provides an advanced environment for experimenting with and developing marine technologies, such as the BlueROV2 and Girona 500 AUV. The water tank at CIRTESU has dimensions of 12m x 8m x 5m, holding half a million liters of water, and offers the necessary infrastructure for conducting detailed experiments. The lab is equipped with systems for control, data acquisition, analysis, and real-time tracking to measure movement in six degrees of freedom (6DOF).

4

Results and Discussions

Contents

4.1 Preliminary Setup

In the Preliminary Setup phase, the LUMA modems were initially tested in air to establish a baseline for their performance in ideal conditions before transitioning to underwater testing. This step was crucial in understanding how the modems handle communication when optical signals are transmitted in an environment devoid of water-based interference.

During these air-based tests, bandwidth graphs were generated by varying the angle of the LUMA modems used for communication. The results demonstrated how signal strength fluctuated in response to changes in angles and distances, providing insights into the modems' performance under different conditions. The bandwidth remained relatively stable in direct line-of-sight communication but decreased when the modems were positioned at steeper angles or when light intensity was reduced. The data revealed that the LUMA modems could maintain a strong connection with minimal signal degradation in optimal lighting conditions. Still, the signal quality decreased as the light source was obstructed or weakened. This initial testing in air allowed us to establish key performance indicators for the LUMA modems and helped to perform adjustments to both the positioning and intensity of light used in subsequent underwater tests.

To perform the experiment, the optical modems were positioned at distances of $3m$, $5m$, $7m$, and $8m$. Initially, the modems were aligned directly facing each other to establish a clear line of sight for optimal communication. Afterward, one modem was moved ± 90 degrees to the right and left to test the impact of angular misalignment on signal strength and bandwidth performance. This approach allowed for the evaluation of both distance and alignment sensitivity in the optical communication setup. The parameter settings for these two optical modems are displayed in table 4.1

Parameter	**Setting**
Auto-power active	Off
Max number of active LEDs	5
Auto-speed active	Off
Optical speed	10 MHz
Encoding	Off
Auto gain control	On - fixed sensitivity

Table 4.1: Parameter Settings of LUMA Modem in Air

The analysis of bandwidth and signal strength plots shows a clear correlation between modem alignment and communication performance. Initially, when the optical modems are aligned, both bandwidth and signal strength remain relatively stable. The signal strength as shown in Figure 4.1 ranges between 700 and 900 units, and the bandwidth stayed close to the 10 Mbps maximum, with minor fluctuations that could be attributed to environmental factors like light interference or slight movements. This indicates that the system performs optimally when the modems are properly aligned, with only minimal variations caused by TCP's natural adjustments for congestion control. However, as soon as the second modem

is moved to ± 90 degrees from the initial alignment, a significant drop in both bandwidth and signal strength occurs. Around the 125-second mark, the signal strength falls from 750 to around 200 units, causing the bandwidth to fluctuate below 10 Mbps. This clearly illustrates that optical communication is highly sensitive to alignment. Misalignment results in a substantial degradation in signal quality, which in turn reduces the available bandwidth and introduces more pronounced fluctuations in the system.

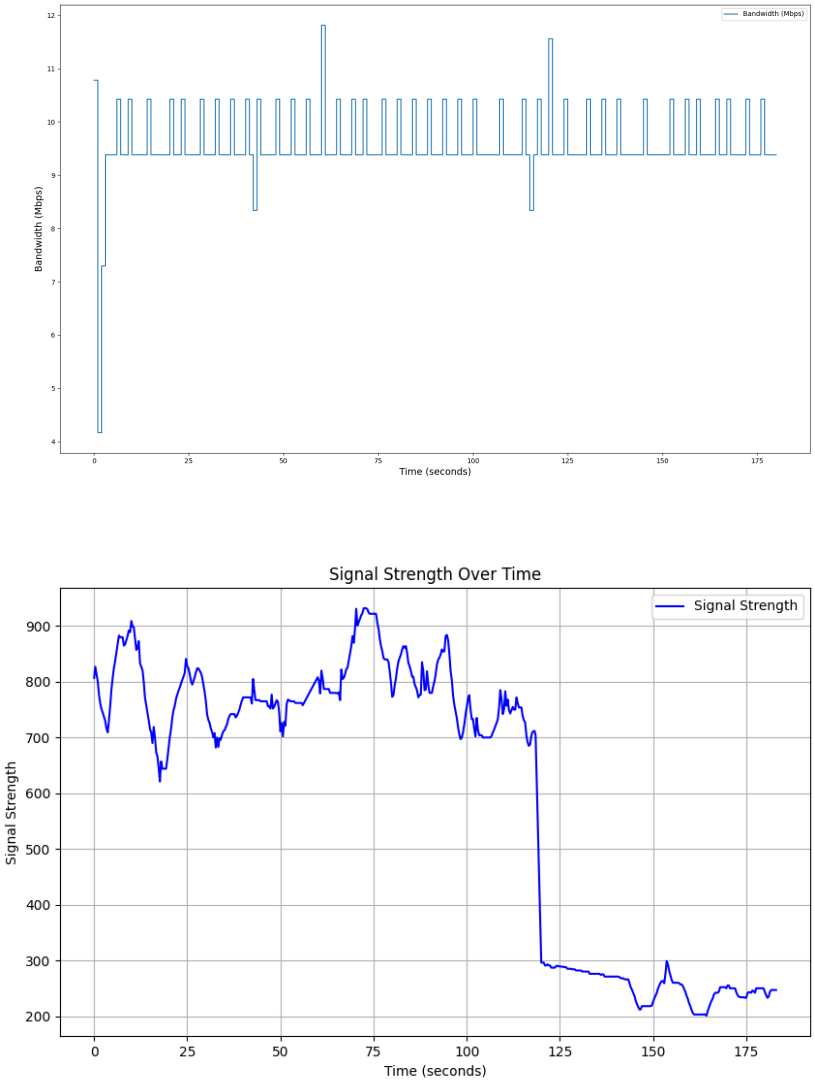

Figure 4.1: Bandwidth and Signal Strength plots at 3-meter distance.

The analysis of the tests conducted at distances of $5m$, $7m$, and $8m$ reveals a clear correlation between distance and the stability of both bandwidth and signal strength. At a 5-meter distance as seen in Figure 4.2, the system maintains an average bandwidth close to 10 Mbps, though fluctuations occur due to variations in signal strength and alignment. The signal strength starts strong but steadily

declines from 1000 units to around 400 units by the end of the test. This decline correlates with drops in bandwidth, particularly around 30 and 60 seconds, where both signal and bandwidth dip briefly. Despite these fluctuations, the system recovers intermittently, showing temporary improvements.

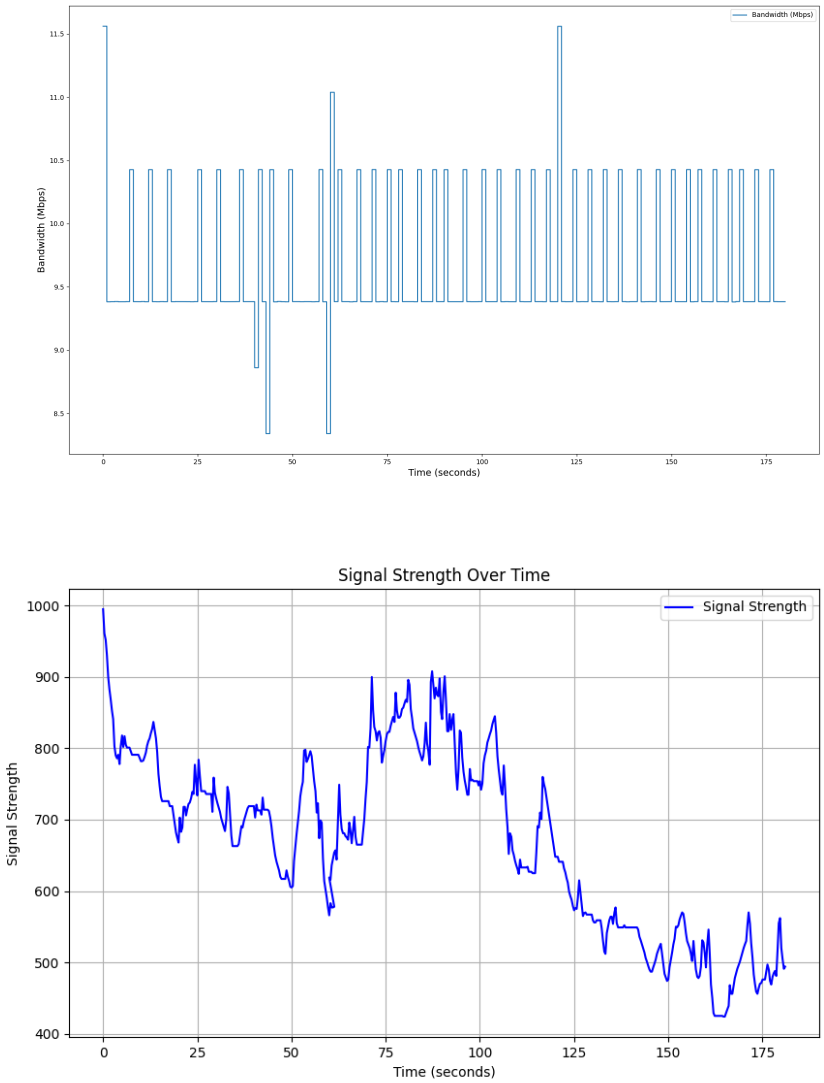

Figure 4.2: Bandwidth and Signal Strength plots at 5-meter distance.

At 7 meters, the optical communication system became more unstable, with frequent drops in both bandwidth and signal strength. The correlation between the dips in signal strength and the drops in bandwidth highlights the increasing sensitivity of the system to alignment and environmental factors as distance increases. The system 4.3 struggles to maintain consistent performance beyond 100 seconds, especially when signal strength drops significantly.

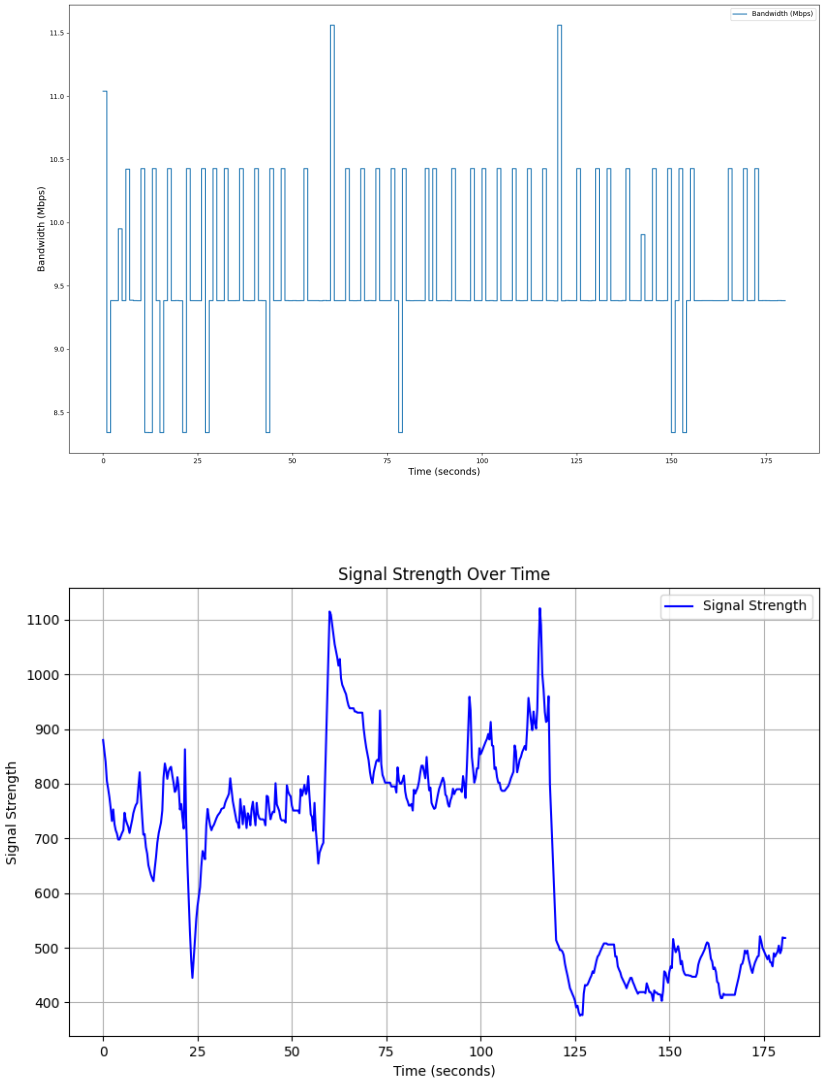

Figure 4.3: Bandwidth and Signal Strength plots at 7-meter distance.

At 8 meters, the plots of, shown in Figure 4.4 bandwidth and signal strength exhibit frequent and deep fluctuations. The large dips in signal strength directly affect bandwidth, causing frequent disruptions and a drop in overall performance. To improve stability at this distance, better alignment or enhanced transmission power would be needed to maintain a reliable optical link.

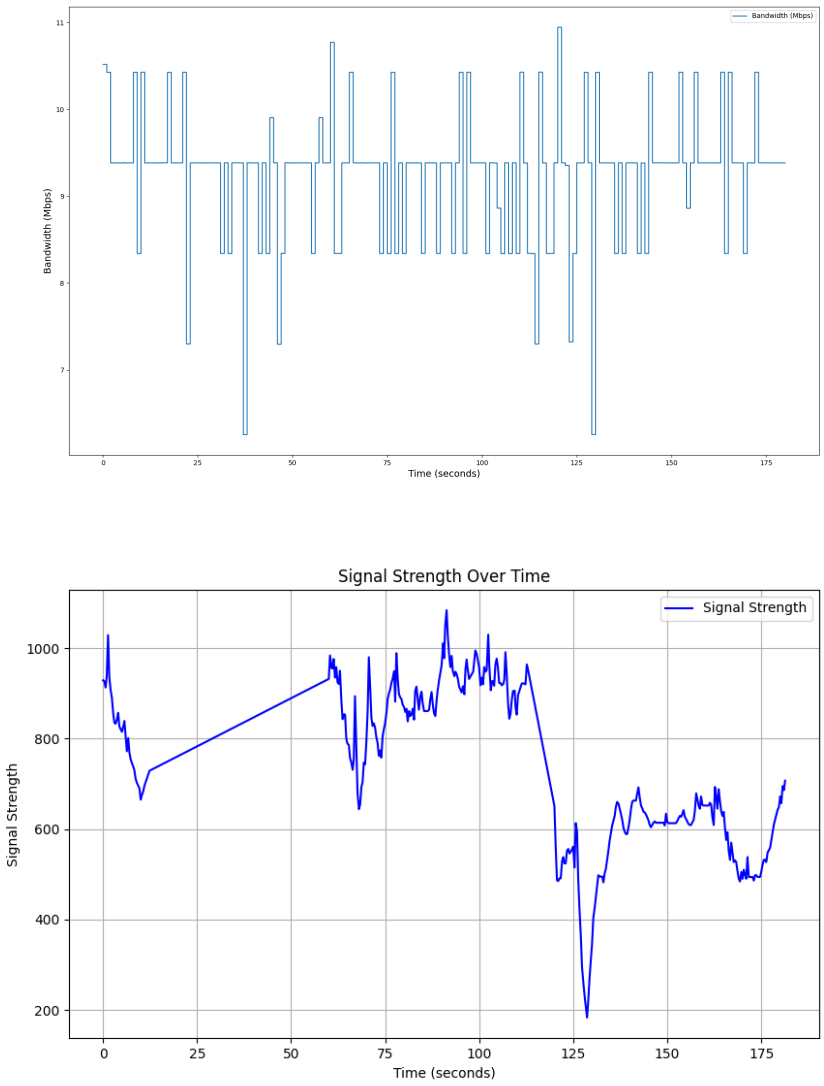

Figure 4.4: Bandwidth and Signal Strength plots at 8-meter distance.

Optical wireless communication relies on a clear, direct path between the transmitter and receiver, and any deviation from this alignment—such as the movement of the second modem to a 90-degree angle—causes the signal to weaken significantly. This leads to lower bandwidth and increased variability, as seen in the plots. Additionally, the behavior of TCP, which tries to adapt to changing network conditions, can exacerbate these fluctuations by briefly increasing bandwidth during re-transmissions or congestion control. Natural light can significantly impact the performance of optical modems by introducing interference and noise, especially when the light overlaps with the wavelengths used by the modems. This interference can lower the signal-to-noise ratio, reduce bandwidth, and cause communication errors. Additionally, natural light can cause scattering and reflection, further degrading the signal.

In the next phase of testing, the LUMA modems were evaluated in a controlled pool environment to move towards more realistic underwater conditions. This setup was designed to assess how the modems performed in water, especially regarding bandwidth, and the ability to communicate between vehicles following different trajectories.

4.2 Pool Testing

The modems were then installed on two remotely operated vehicles (ROVs), with one acting as the leader and the other as the follower. The leader ROV was responsible for sending its real-time pose data—such as position and orientation—via the LUMA modem to the follower vehicle. To ensure effective data transmission, several trajectories were designed and tested. These trajectories varied in complexity, from straight-line movements to more dynamic paths involving turns and varying speeds. Each scenario provided valuable insights into the reliability of the optical communication link under different movement conditions. To save power and transmit pose of the leader vehicle, the modems were tested with an optical speed of 6 Mhz. The other parameters were kept same as shown in table 4.2.

Parameter	**Setting**
Auto-power active	Off
Max number of active LEDs	5
Auto-speed active	Off
Optical speed	6 MHz
Encoding	Off
Auto gain control	On - fixed sensitivity

Table 4.2: Parameter Settings of LUMA Modem in Water

The bandwidth was continuously monitored as the follower vehicle moved along its designated trajectory. The modems effectively maintained a stable communication link during simpler trajectories, such as straight-line movements, where the vehicles remained within a clear line of sight. However, in more complex paths, such as those involving turns or shifts in depth, signal degradation was observed due to

factors like alignment loss or light scattering in water.

Despite these challenges, the modems on the leader vehicle were able to send accurate and timely pose data to the follower vehicle. This confirmed the viability of the optical communication link for real-time coordination in leader-follower systems. The testing also highlighted the importance of careful modem placement and trajectory planning to minimize communication disruptions in underwater environments. Figure 4.5 shows the plots of bandwidth and leaders' pose in x,y,z directions that followed a straight-line trajectory. The blue line represents yaw angles. The measurements are taken in meters.

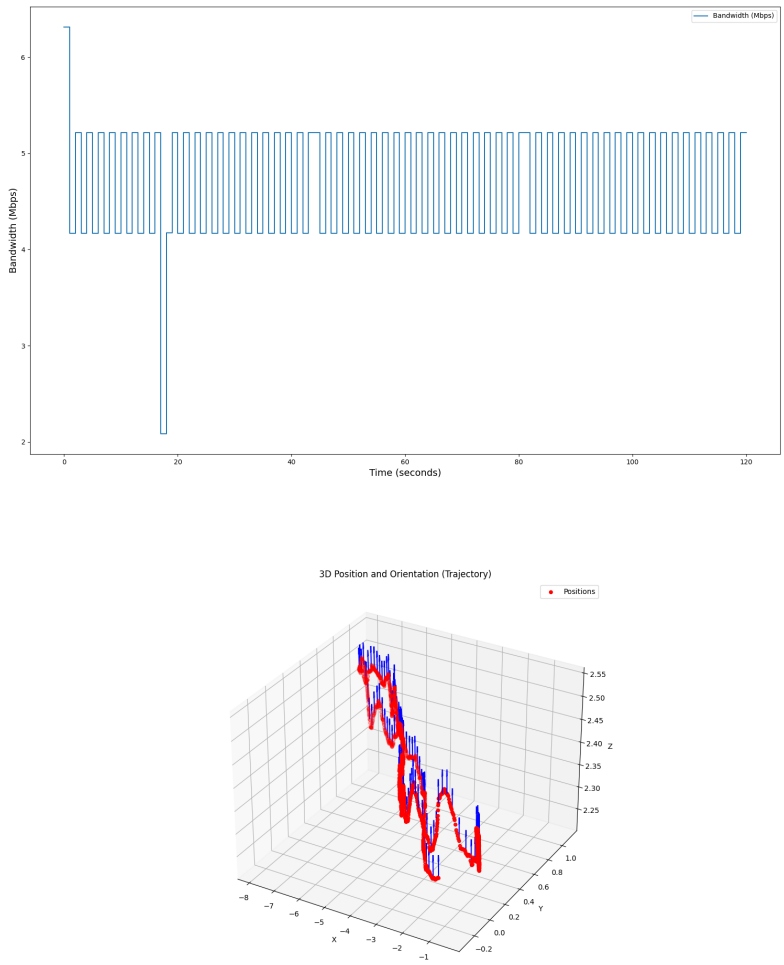

Figure 4.5: Follower Vehicle Bandwidth Response and Leader ROV Pose for a simple trajectory.

The 3D position and orientation plot shown in Figure 4.6 shows that the leader vehicle followed a complex trajectory, which was successfully transmitted to the follower vehicle. The red dots representing the positions show a continuous and smooth data flow in real-time, despite the dynamic movements

and changes in the trajectory. This reflects the system's ability to transmit not just static positions but dynamic motion effectively.

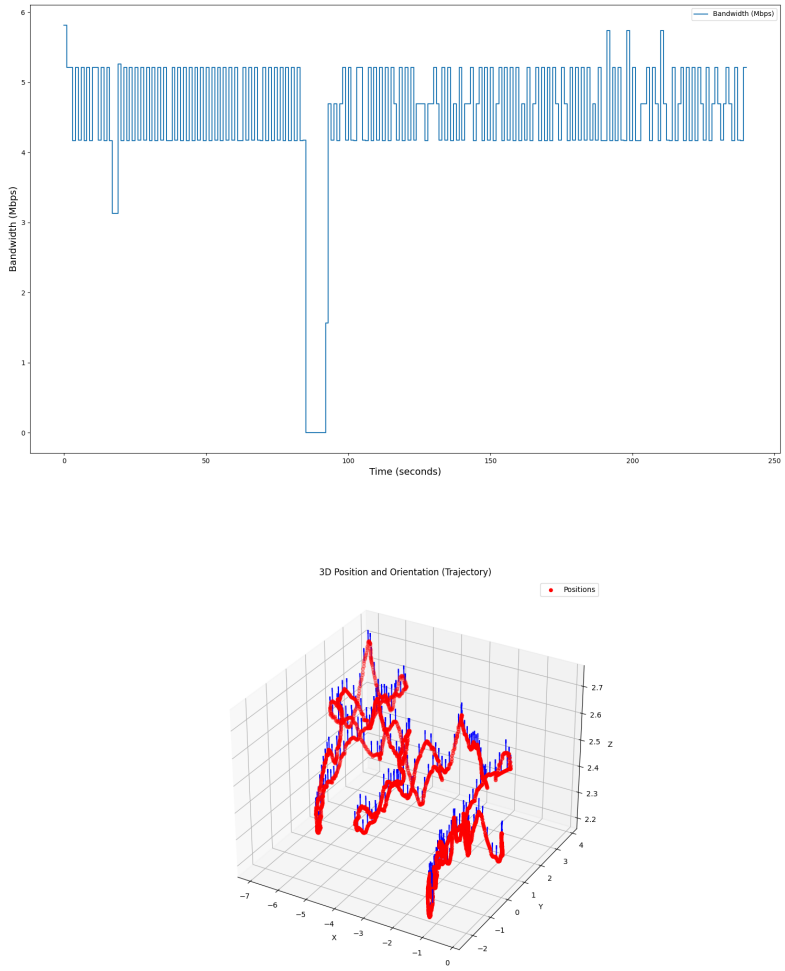

Figure 4.6: Follower Vehicle Bandwidth Response and Leader ROV Pose for a Complex Trajectory.

Some more complex trajectories, particularly when the leader vehicle moved farther away, showed that the optical modem struggled to maintain a stable link, ultimately reaching the operational limits of the modem's range. The frequent drops in bandwidth and instances of lost communication indicate that the optical link becomes unreliable at greater distances. While some data was still transmitted, the performance significantly degraded, with large gaps in both the pose and bandwidth plots as shown in Figure 4.7 and 4.8. To improve communication stability at such long ranges, optical speed must be reduced since a higher optical speed means less range and less resilience to optical noise and ambient light. .

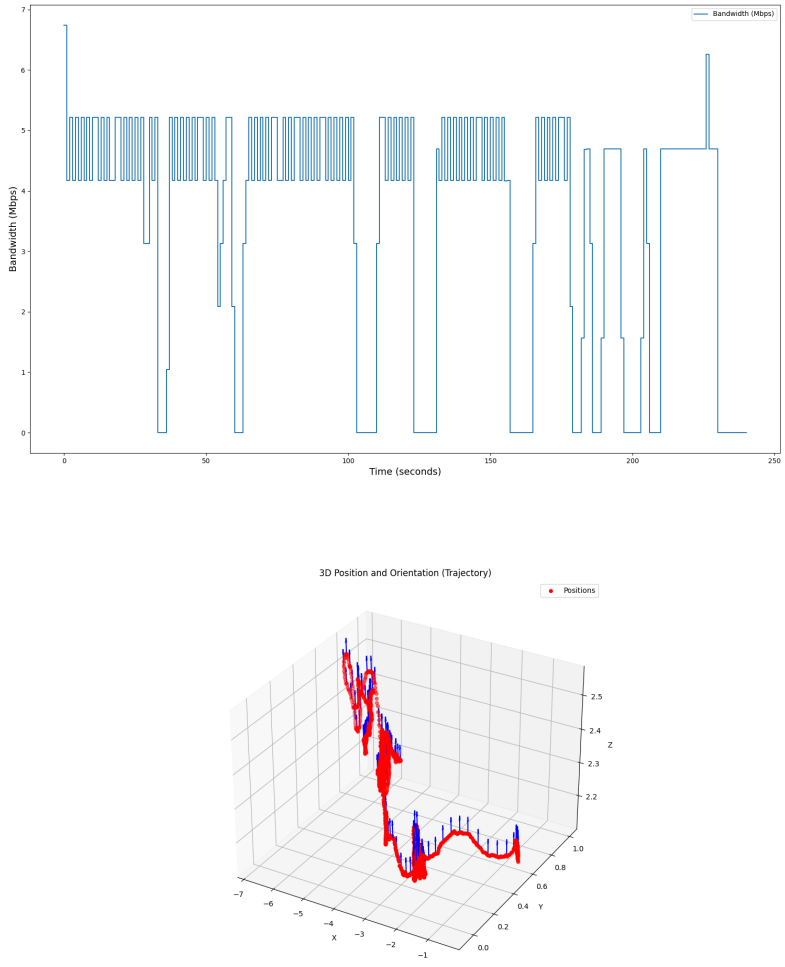

Figure 4.7: Follower Vehicle Bandwidth Response and Leader ROV Pose Reaching the Operational Limits of Modems

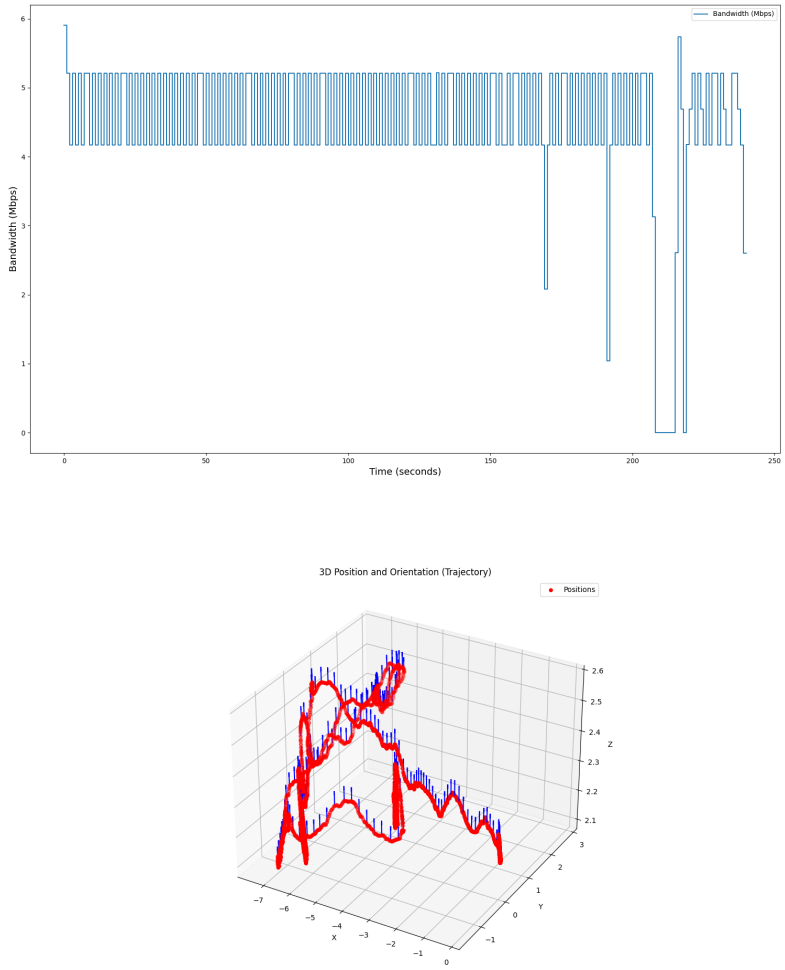

Figure 4.8: Follower Vehicle Bandwidth Response and Leader ROV Pose.

4.3 Leader-Follower Controller Analysis

This section presents the analysis of the leader-follower controller designed using the state-space model and matrices defined earlier. The objective of the leader-follower system is to ensure that the follower accurately maintains a fixed relative position from the leader over time while dealing with external disturbances and maintaining control stability. The system is implemented using MATLAB, and the feedback control protocol is designed to achieve synchronization between the leader and the follower.

The goal of this simulation is to evaluate the closed-loop performance of the leader-follower system under the proposed feedback control law. The system is subjected to disturbances through matrix E

and the follower must use feedback control to track the leader while minimizing the effects of these disturbances.

Since the physical implementation on the BlueROV2 was not feasible due to limited time, the state-space model was used to simulate and analyze the controller. The simulation was carried out in MATLAB, where the leader and follower dynamics were modeled using the state-space representation described earlier. The control inputs, disturbances, and feedback gains were applied to evaluate how effectively the follower tracks the leader's state.

Using the dynamic feedback protocol from Equation (3.19), the feedback gain matrices *F* and *G* were computed to achieve leader-follower consensus. The gain matrices are computed by solving the algebraic Riccati inequality, ensuring the system's stability and minimizing the H_2 cost function. For this simulation, the guidelines from [48] are followed to compute the gain matrices:

$$F = \begin{bmatrix} -5.7580 & -1.4146 & -0.9958 & -1.5151 \end{bmatrix}$$

and,

$$G = \begin{bmatrix} 0.0354 \\ 0.3569 \\ 0.0374 \\ 0.0633 \end{bmatrix}$$

The cost function J(F,G) is calculated to ensure that the system operates below the desired upper bound. By solving the Riccati inequality and using the MATLAB command `norm(sys,2)`, the norm of the controlled error system is calculated as $h_{F,G} = 1.2825$ which is less than $\sqrt{\gamma} = 1.3053$. This indicates that the proposed controller is effective and operates within the desired performance bounds.

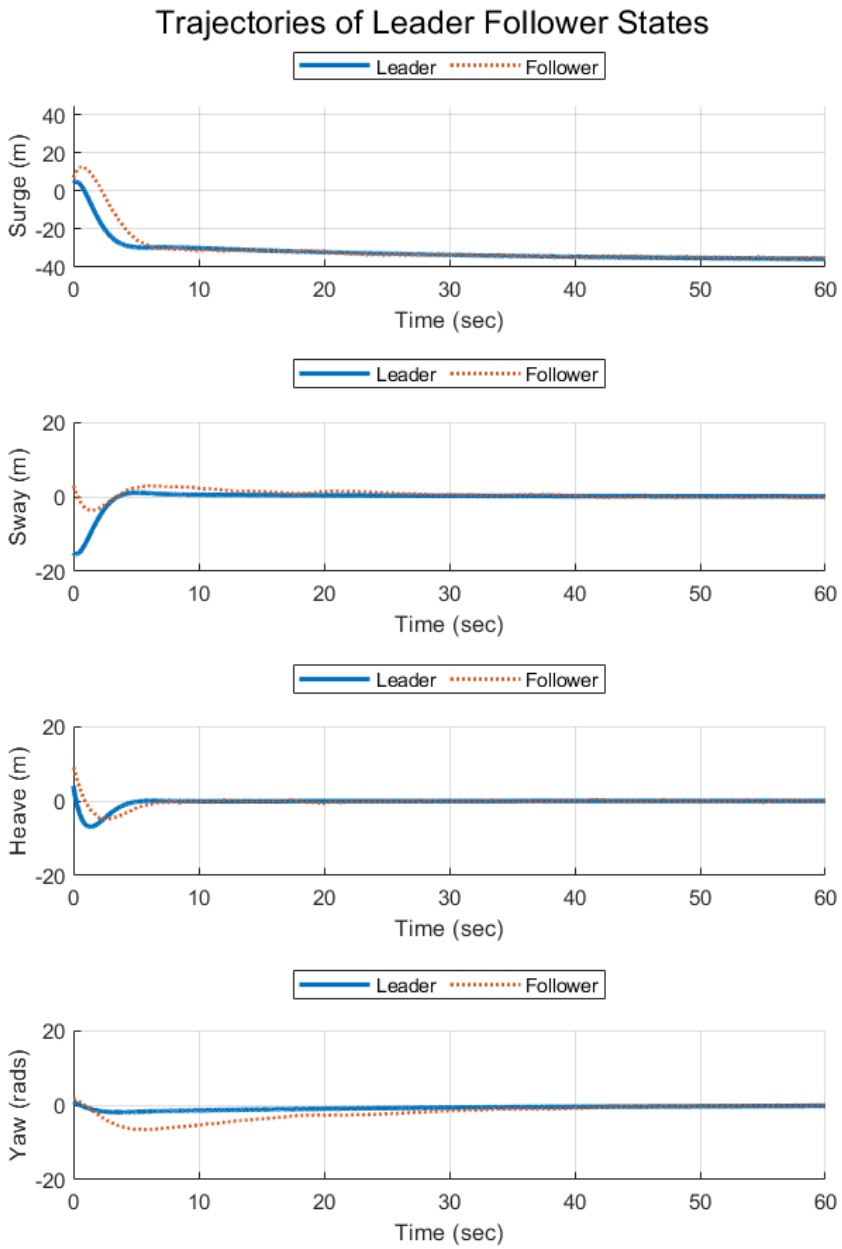

Figure 4.9: Trajectories of States.

Figure 4.9 shows the trajectory of the states of both leader and follower. The simulation demonstrates that the follower achieves synchronization with the leader. The performance output $z_i(t) - z_l(t)$ as seen in Figure 4.10, representing the difference between the follower's and leader's outputs, converges to zero as time progresses.

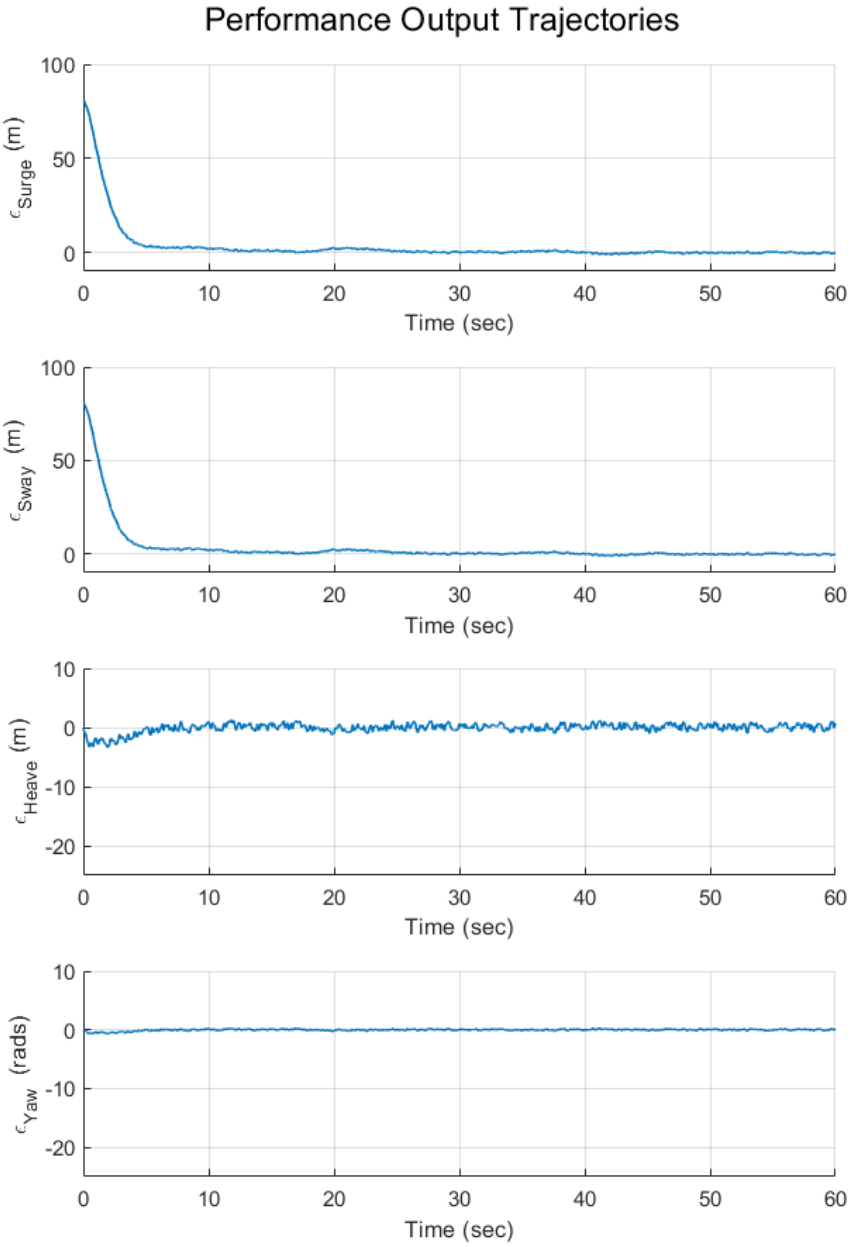

Figure 4.10: Performance Output Trajectories.

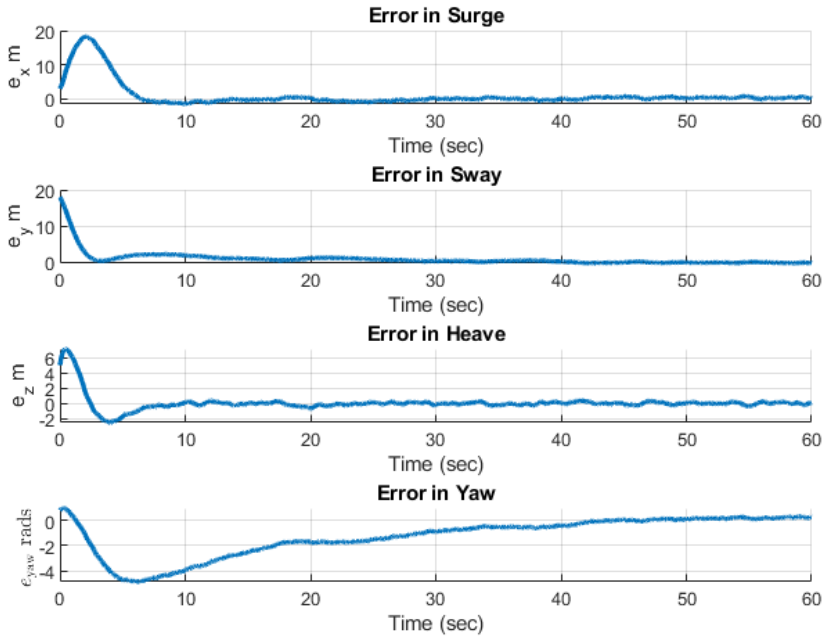

Figure 4.11: Error State for the Follower.

The system was subjected to white noise d with an amplitude ranging between -15 and 15, applied to the follower. The simulation results validate the proposed leader-follower controller using the state-space model. The feedback control law ensures system stability, disturbance rejection, and convergence to the leader's state, even though the implementation of the controller on BlueROV2 was not possible. Figure 4.11 shows that the controller was able to effectively minimize the error between the leader and follower states, thereby reaching synchronization. The MATLAB simulation demonstrates the robustness of the controller design, highlighting its potential for real-world applications in leader-follower multi-agent systems.

4.4 Discussions

The MATLAB simulation demonstrates that the follower achieves synchronization with the leader. The performance output $\epsilon = z_i - z_l$, which represents the difference between the follower's and leader's outputs, converges to zero as time progresses.

Due to the limited time, the controller could not be implemented directly on the BlueROV2 platform using ROS. As a result, a state-space model of the leader-follower dynamics was used to evaluate the performance of the proposed controller. Despite the limitations of not using the actual hardware, the MATLAB simulations provide a reliable evaluation of the controller's effectiveness.

The leader-follower controller design effectively controls the follower vehicle, enabling it to track the leader's state with minimal error. The state-space matrices used in this design, along with the feedback gain matrices G and F, ensure that the system is controllable, observable, and robust to disturbances. The MATLAB simulations validate the system's performance, showcasing that the follower can accurately track the leader while mitigating the impact of external disturbances

The results validate the effectiveness of the proposed leader-follower controller. The simulation demonstrates that the control inputs successfully guide the follower vehicle to align its state with the leader's state. The design also ensures that external disturbances are compensated, ensuring smooth operation. The performance analysis reveals that the leader-follower controller can be applied to a wide range of applications in marine robotics, specifically for multi-agent systems requiring robust communication and control mechanisms.

5

Conclusion

Contents

5.1 Conclusion

This thesis highlights the successful development and validation of a leader-follower control strategy for underwater multi-agent system using LUMA™optical modems for communication. The proposed framework, validated through MATLAB simulations, demonstrated effective underwater coordination. The MATLAB simulations confirmed the robustness and accuracy of the control strategy under idealized conditions, showing that the follower could effectively maintain formation with the leader. It is important to note that the simulations were not conducted using the BlueROV2 simulator, which limits the direct applicability of the results to the real vehicle without further testing. This research contributes to the field of underwater robotics by providing a reliable framework for coordinated control of multiple autonomous vehicles using high-speed optical communication links. The results indicate that optical communication can effectively solve precise underwater vehicle coordination, offering high data rates and minimal latency. Since we have high data rates and minimal latency the communication system is considered ideal and doesn't need to be modeled in MATLAB.

5.2 Future Work

Several avenues of research and development are essential to enhance the robustness and practicality of the proposed leader-follower control system using optical modems for underwater autonomous vehicles. Below are key directions for future work:

- **Testing Using Unity Simulator**

  If time were not a constraint, Unity could be utilized to provide a powerful and flexible simulation environment for testing the proposed control system. This approach would allow for an in-depth evaluation of the system's performance under a wide range of underwater conditions, without the limitations posed by physical testing setups or time restrictions. Unity's capabilities include the simulation of intricate underwater dynamics, such as vehicle interactions with ocean currents, small turbulence effects, and environmental disturbances, enabling comprehensive testing of precision, robustness, and reliability in a controlled, virtual setting. With Unity, it would be possible to visualize the leader-follower behavior in real time, which would enhance the understanding of control strategies and communication dynamics. Additionally, Unity's versatility would allow for iterative improvements and the fine-tuning of control algorithms, potentially leading to significant performance optimizations and insights that may be challenging to obtain in physical tests alone. This expanded simulation framework could pave the way for more advanced testing scenarios and lay a robust groundwork for future experimental applications.

- **Integration of Obstacle Avoidance Mechanisms**

In practical underwater environments, the presence of obstacles and complex terrain is inevitable, posing significant risks to the safe navigation of autonomous vehicles. Future iterations of this control framework must integrate obstacle avoidance algorithms to ensure collision-free operation. The introduction of artificial potential field methods, or behavior-based strategies for obstacle detection and avoidance, will further improve the resilience and applicability of the controller in real-world missions.

- **Expansion to Multiple Follower Agents**

  The expansion of the current system to accommodate multiple follower agents is also a crucial area for further exploration. The leader-follower structure can be extended to involve multiple autonomous vehicles, which will require the development of advanced coordination algorithms to maintain formation and prevent inter-vehicle collisions. This multi-agent extension will be particularly beneficial for large-scale underwater missions that demand coordinated operations among several vehicles.

- **Testing the Controller Using LUMA Modems on BlueROV2**

  Testing the proposed leader-follower controller on BlueROV2 vehicles using LUMA™ optical modems is a critical next step, especially by leveraging a ROS-based environment with Python, as this approach aligns with the LUMA packages, which are developed within the ROS framework. Integrating the controller with LUMA modems in ROS will streamline development and enhance compatibility, making it easier to test the controller's effectiveness directly on the BlueROV2 platform. This setup bypasses MATLAB, reducing potential integration challenges and allowing for more efficient communication handling and data transfer between the modems and the controller. By testing in this configuration, we can validate the controller's feasibility and robustness in an actual underwater environment, where factors such as water clarity, pressure, and ambient light could affect communication performance. This testing phase will offer valuable, real-world insights into underwater communication and control dynamics, essential for assessing the controller's practical viability and refining it for future deployments..

Bibliography

[1] A. Azad, G. Virk, M. Qi, G. Muscato, S. Guccione, G. Nunnari, T. White, C. Glazebrook, A. Semerano, M. Ghrissi, P. Briole, C. Faucher, M. Coltelli, G. Puglisi, R. Cioni, and M. Pompilio, "Robovolc: Remote inspection for volcanoes," in *International NAISO Congress on Information Science Innovations (ISI'2001)*, Dubai, 2001.

[2] O. Schofield, J. Kohut, and S. Glenn, "Using webb gliders to maintain a sustained ocean presence," in *EEE Proceedings of Security and Sensing Symposium*, 2009.

[3] B. Bethke, "Persistent vision-based search and track using multiple uavs," MSc thesis, Massachusetts Institute of Technology - Dept. of Aeronautics and Astronautics, Cambridge, MA, USA, 2005.

[4] GREX, "The grex project: Coordination and control of cooperating heterogeneous unmanned systems in uncertain environments," 2006–2009, http://www.grex-project.eu.

[5] A. Aguiar, J. Almeida, M. Bayat, B. Cardeira, R. Cunha, A. Hausler, P. Maurya, A. Oliveira, A. Pascoal, A. Pereira, M. Rufino, L. Sebastião, C. Silvestre, and F. Vanni, "Cooperative autonomous marine vehicle motion control in the scope of the eu-grex project: Theory and practice," Instituto Superior Técnico - Institute for Systems and Robotics (IST/ISR), Lisbon, Portugal, Technical report, 2009.

[6] R. Ghabcheloo, A. Aguiar, A. Pascoal, C. Silvestre, I. Kaminer, and J. Hespanha, "Coordinated path-following in the presence of communication losses and time delays," *SIAM Journal on Control and Optimization*, vol. 48, no. 1, pp. 234–265, 2009.

[7] J.-H. Li, P.-M. Lee, and Sang-Jeong-Lee, "Neural net based nonlinear adaptive control for autonomous underwater vehicles," in *Proceedings 2002 IEEE International Conference on Robotics and Automation (Cat. No.02CH37292)*, vol. 2, 2002, pp. 1075–1080 vol.2.

[8] S. López-Barajas, P. J. Sanz, R. Marín-Prades, A. Gómez-Espinosa, J. González-García, and J. Echagüe, "Inspection operations and hole detection in fish net cages through a hybrid

underwater intervention system using deep learning techniques," *Journal of Marine Science and Engineering*, vol. 12, no. 1, 2024. [Online]. Available: https://www.mdpi.com/2077-1312/12/1/80

[9] X. Lin, W. Tian, W. Zhang, J. Zeng, and Y. Liu, "Fault-tolerant consensus of leaderless multi-auv system with partial actuator breakdown," in *2021 33rd Chinese Control and Decision Conference (CCDC)*, 2021, pp. 3181–3186.

[10] M. J. Er, H. Gong, Y. Liu, and T. Liu, "Intelligent trajectory tracking and formation control of underactuated autonomous underwater vehicles: A critical review," *IEEE Transactions on Systems, Man, and Cybernetics: Systems*, vol. 54, no. 1, pp. 543–555, 2024.

[11] C. Shen, Y. Shi, and B. Buckham, "Lyapunov-based model predictive control for dynamic positioning of autonomous underwater vehicles," in *2017 IEEE International Conference on Unmanned Systems (ICUS)*, 2017, pp. 588–593.

[12] K. Sathish, C. V. Ravikumar, A. Rajesh, and G. Pau, "Underwater wireless sensor network performance analysis using diverse routing protocols," *Journal of Sensor and Actuator Networks*, vol. 11, no. 4, 2022. [Online]. Available: https://www.mdpi.com/2224-2708/11/4/64

[13] J. Kalwa, A. Pascoal, P. Ridao, A. Birk, T. Glotzbach, L. Brignone, M. Bibuli, J. Alves, and M. Silva, "Eu project morph: Current status after 3 years of cooperation under and above water," *IFAC-PapersOnLine*, vol. 48, no. 2, p. 119–124, 2015, 4th IFAC Workshop on Navigation, Guidance and Control of Underwater Vehicles (NGCUV 2015).

[14] G. Indiveri, G. Antonelli, F. Arrichiello, A. Caffaz, A. Caiti, G. Casalino, N. C. Volpi, I. B. de Jong, D. D. Palma, H. Duarte, J. P. Gomes, J. Grimsdale, S. Jesus, K. Kebkal, E. Kelholt, A. Pascoal, D. Polani, L. Pollini, E. Simetti, and A. Turetta, "Overview and first year progress of the widely scalable mobile underwater sonar technology h2020 project—this work has received funding from the european union's horizon 2020 research and innovation programme under grant agreement no. 645141 (wimust project, http://www.wimust.eu)," *IFAC-PapersOnLine*, vol. 49, no. 23, p. 430–433, 2016, 10th IFAC Conference on Control Applications in Marine Systems (CAMS 2016).

[15] S. Fattah, A. Gani, I. Ahmedy, M. Y. I. Idris, and I. A. Targio Hashem, "A survey on underwater wireless sensor networks: Requirements, taxonomy, recent advances, and open research challenges," *Sensors*, vol. 20, no. 18, 2020. [Online]. Available: https://www.mdpi.com/1424-8220/20/18/5393

[16] M. Jouhari, K. Ibrahimi, H. Tembine, and J. Ben-Othman, "Underwater wireless sensor networks: A survey on enabling technologies, localization protocols, and internet of underwater things," *IEEE Access*, vol. 7, pp. 96 879–96 899, 2019.

[17] A. Patil, M. Park, and J. Bae, “Coordinating tethered autonomous underwater vehicles towards entanglement-free navigation,” *Robotics*, vol. 12, no. 3, 2023. [Online]. Available: https://www.mdpi.com/2218-6581/12/3/85

[18] I. Vasilescu, P. Varshavskaya, K. Kotay, and D. Rus, “Autonomous modular optical underwater robot (amour): Design, prototype and feasibility study,” in *Proc. IEEE International Conference on Robotics and Automation (ICRA’05)*, Barcelona, Spain, Apr. 2005, p. 1603–1609, pages 47, 53.

[19] M. Dunbabin, J. Roberts, K. Usher, G. Winstanley, and P. Corke, “A hybrid auv design for shallow water reef navigation,” in *Proc. IEEE International Conference on Robotics and Automation (ICRA’05)*, Barcelona, Spain, Apr. 2005, p. 2105–2110, pages 48.

[20] B. Tian, F. Zhang, and X. Tan, “Design and development of an led-based optical communication system for autonomous underwater robots,” in *Proc. IEEE/ASME International Conference on Advanced Intelligent Mechatronics (AIM’13)*, Wollongong, Australia, Jul. 2013, p. 1558–1563, pages 48.

[21] M. Tabacchiera, S. Betti, and S. Persia, “Underwater optical communications for swarm unmanned vehicle network,” in *Proc. Fotonica AEIT Italian Conference on Photonics Technologies*, Naples, Italy, May 2014, p. 1–3, pages 48, 53.

[22] Z. Zeng, S. Fu, H. Zhang, Y. Dong, and J. Cheng, “A survey of underwater optical wireless communications,” *IEEE Communications Surveys & Tutorials*, vol. 19, no. 1, pp. 204–238, 2017.

[23] C. Pontbriand, N. E. Farr, J. D. Ware, J. C. Preisig, and H. L. Popenoe, “Diffuse high-bandwidth optical communications,” in *OCEANS*, 2008, pp. 1–4.

[24] P. G. Goetz, W. S. Rabinovich, R. Mahon, J. L. Murphy, M. S. Ferraro, M. R. Suite *et al.*, “Modulating retro-reflector lasercom systems for small unmanned vehicles,” *IEEE Journal on Selected Areas in Communications*, vol. 30, no. 5, pp. 986–992, 2012.

[25] S. Arnon and D. Kedar, “Non-line-of-sight underwater optical wireless communication network,” *J. Opt. Soc. Am. A*, vol. 26, no. 3, pp. 530–539, March 2009.

[26] M. Kong, W. Lv, T. Ali, R. Sarwar, C. Yu, Y. Qiu *et al.*, “10-m 9.51-gb/s rgb laser diodes-based wdm underwater wireless optical communication,” *Optics Express*, vol. 25, no. 17, pp. 20 829–20 834, August 2017.

[27] J. Shen, J. Wang, C. Yu, X. Chen, J. Wu, M. Zhao *et al.*, “Single led-based 46-m underwater wireless optical communication enabled by a multi-pixel photon counter with digital output,” *Optics Communications*, vol. 438, pp. 78–82, 2019.

[28] H.-H. Lu, C.-Y. Li, X.-H. Huang, P.-S. Chang, Y.-T. Chen, Y.-Y. Lin *et al.*, "A 400-gb/s wdm-pam4 owc system through the free-space transmission with a water–air–water link," *Scientific Reports*, vol. 11, no. 1, p. 21431, November 2021.

[29] C.-Y. Li, H.-H. Lu, Y.-C. Wang, Z.-H. Wang, C.-W. Su, Y.-F. Lu *et al.*, "An 82-m 9 gb/s pam4 fso-pof-uwoc convergent system," *IEEE Photonics Journal*, vol. 11, no. 1, pp. 1–9, 2019.

[30] W.-S. Tsai, H.-H. Lu, H.-W. Wu, S.-C. Tu, Y.-C. Huang, J.-Y. Xie *et al.*, "500 gb/s pam4 fso-uwoc convergent system with a r/g/b five-wavelength polarization-multiplexing scheme," *IEEE Access*, vol. 8, pp. 16 913–16 921, 2020.

[31] H. Chen, X. Chen, J. Lu, X. Liu, J. Shi, L. Zheng *et al.*, "Toward long-distance underwater wireless optical communication based on a high-sensitivity single photon avalanche diode," *IEEE Photonics Journal*, vol. 12, no. 3, pp. 1–10, 2020.

[32] N. Saeed, A. Celik, T. Y. Al-Naffouri, and M.-S. Alouini, "Underwater optical wireless communications networking and localization: A survey," *Ad Hoc Networks*, vol. 94, p. 101935, 2019.

[33] S. Arnon, "Underwater optical wireless communication network," *Optical Engineering*, vol. 49, no. 1, p. 015001, 2010.

[34] Hydromea, "Luma underwater communication."

[35] S. Emrani, A. Dirafzoon, and H. A. Talebi, "Leader-follower formation control of autonomous underwater vehicles with limited communications," in *2011 IEEE International Conference on Control Applications (CCA)*, 2011, pp. 921–926.

[36] C. H. Fua, S. S. Ge, K. D. Do, and K. W. Lim, "Multirobot formations based on the queue-formation scheme with limited communication," *IEEE Transactions on Robotics*, vol. 23, no. 6, pp. 1160–1169, 2007.

[37] M. A. Lewis and K. H. Tan, "High precision formation control of mobile robots using virtual structures," *Autonomous Robots*, vol. 4, no. 4, pp. 387–403, 1997.

[38] T. Balch and R. C. Arkin, "Behavior-based formation control for multirobot teams," *IEEE Transactions on Robotics and Automation*, vol. 14, no. 6, pp. 926–939, 1998.

[39] S. S. Ge and C. H. Fua, "Queues and artificial potential trenches for multirobot formations," *IEEE Transactions on Robotics*, vol. 21, no. 4, pp. 646–656, 2004.

[40] N. Yang, M. Reza Amini, M. Johnson-Roberson, and J. Sun, "Real-time model predictive control for energy management in autonomous underwater vehicle," in *2018 IEEE Conference on Decision and Control (CDC)*, 2018, pp. 4321–4326.

[41] T. I. Fossen, *Handbook of Marine Craft Hydrodynamics and Motion Control*. John Wiley & Sons, 2011.

[42] X. Zhang, K. Ma, Y. Wei, and Y. Han, "Finite-time robust h_∞ control for high-speed underwater vehicles subject to parametric uncertainties and disturbances," *Journal of Marine Science and Technology*, vol. 22, no. 2, pp. 201–218, 2017.

[43] Y. Wang, L. Bai, and S. Liu, "Robust h_2/h_∞ control of nonlinear system with differential uncertainty," in *Proceedings of the 2014 IEEE Conference and Expo Transportation Electrification Asia-Pacific (ITEC Asia-Pacific)*, 2014, pp. 1–6.

[44] T. SNAME, "Nomenclature for treating the motion of a submerged body through a fluid," *The Society of Naval Architects and Marine Engineers, Technical and Research Bulletin*, no. 1950, pp. 1–5, 1950.

[45] X. Wu, "Underwater optical wireless communication systems: Design, modelling and performance analysis," Ph.D. dissertation, Flinders University, 2018.

[46] B. Mokleiv, "Fault-tolerant observer design," Master's thesis, NTNU, 2017.

[47] H. L. Trentelman, K. Takaba, and N. Monshizadeh, "Robust synchronization of uncertain linear multi-agent systems," *IEEE Transactions on Automatic Control*, vol. 58, no. 6, pp. 1511–1523, 2013.

[48] J. Jiao, H. L. Trentelman, and M. K. Camlibel, "A suboptimality approach to distributed h2 control by dynamic output feedback," *Automatica*, vol. 121, p. 109164, 2020. [Online]. Available: https://www.sciencedirect.com/science/article/pii/S0005109820303629

[49] ROS, "Ros," 2007, ros.org [Accessed: 04.12.2023].

A

Code of Project

A.1 Code to Update LUMA Parameters

```
import rospy
import requests
from luma_modem.srv import ChangeParameters, ChangeParametersResponse

#url = 'http://192.168.1.112/api/parameters.json'
def fetch_parameters(ip_suffix):
    url = f'http://192.168.1.{ip_suffix}/api/parameters.json'
    response = requests.get(url)
    if response.status_code == 200:
        return response.json()
    else:
        rospy.logerr("Failed to fetch JSON file. Status code: %d", response.status_code)
        return None


def update_ros_parameters(parameters):
```

```
    if parameters:
        rospy.set_param('/my_parameters/optical_speed', parameters['optical_speed'])
        rospy.set_param('/my_parameters/nb_led', parameters['nb_led'])
        rospy.set_param('/my_parameters/auto_power', parameters['auto_power'])
        rospy.set_param('/my_parameters/auto_speed', parameters['auto_speed'])
        rospy.set_param('/my_parameters/encoding', parameters['encoding'])
        rospy.loginfo("Parameters updated on ROS parameter server.")
    else:
        rospy.logerr("Failed to fetch updated parameters.")
```

A.2 Code to Observe Signal Strength

```
import rospy
from luma_modem.msg import NameValueArray  # Custom message type for name-value pairs
import requests
import numpy as np

def get_last_three_digits(ip_suffix):
    return ip_suffix

def publish_data(ip_suffix):
    # Initialize ROS node
    rospy.init_node('luma_status_publisher', anonymous=True)
    rate = rospy.Rate(3)  # 3 Hz
    # Publisher to publish the custom message
    pub = rospy.Publisher('luma_status', NameValueArray, queue_size=10)
    while not rospy.is_shutdown():
        url = f'http://192.168.1.{ip_suffix}/api/status.json'
        #rospy.loginfo(f"Attempting to fetch data from URL: {url}")  # Debug statement
        response = requests.get(url)
        if response.status_code == 200:
            #rospy.loginfo("Received successful response from server")  # Debug statement
            json_data = response.json()
            names = []
            values = []
            for key, value in json_data.items():
                names.append(key)
                values.append(np.float32(value))  # Convert value to float32
            # Create custom message
            name_value_msg = NameValueArray()
            name_value_msg.names = names
            name_value_msg.values = values
            # Publish the message
            pub.publish(name_value_msg)
```

```
            #rospy.loginfo("Published message to data_topic")  # Debug statement
        else:
            rospy.logerr(f"Failed to fetch JSON file. Status code: {response.status_code}")  # Error message
        rate.sleep()

if __name__ == '__main__':
    try:
        ip_suffix = rospy.get_param('/luma_status_publisher/ip_suffix', 1)  # Get ip_suffix parameter from the ROS parameter server
        rospy.loginfo(f"Using IP suffix: {ip_suffix}")  # Debug statement
        publish_data(ip_suffix)
    except rospy.ROSInterruptException:
        rospy.logwarn("ROSInterruptException occurred")  # Debug statement
```